

Dear Editor,

we would like to inform you that a model bug was found during the time of the revision of the manuscript. The MESSy community fixed the bug and we rerun the simulations. The results were not significantly affected by the bug. Nevertheless, for the revised version of the manuscript, we redid the computations and the plots using the new simulations.

Moreover, Dr. Odran Sourdeval joined this work and contributed as a new coauthor of this manuscript.

The manuscript underwent major revisions, therefore, we listed below only the most important changes:

- new section (section 4) regarding the comparison between model ICNC and satellite observations, including two new figures (Figs. 1, 2);
- new subsection (subsection 5.1) for the new analysis required by the Referees, including two new figures (Figs. 3, 4);
- two new test simulations;
- description and new analysis of the numerical tendencies;
- new analysis regarding global warming effects on the tendencies (in subsection 5.5.2, with the new Fig. 10).

Other parts of the manuscript have been revised and updated:

- the Abstract;
- the description of the simulations (section 3);
- the analysis in section 5 (now performed using 5-year simulations instead of 1-year simulations);
- the Conclusions.

Please, find below our point-by-point response to the reviews and the marked-up manuscript version ("latexdiff") at the end of this document.

Thank you very much!

Yours faithfully,

Sara Bacer

# Authors' reply to Referee #1

## General Comments

### *I) Mass microphysical rates*

*Why did you include only the number and not the mass rates in your analysis? The title suggests you are studying both mass and number rates. By including mass rates would be easier to get a more complete picture of how your model works. I assume the mass rate hierarchy could look quite different from the number rate hierarchy.*

Since our previous study (Bacer et al. 2018), we have focused on the number concentration of ice crystals (ICs). This work follows up on the same direction, therefore, only the rates of ICNCs have been identified in the CLOUD submodel, saved, and analysed. Currently, the mass rates are not output variables, and it is not possible to include them in our analysis. We agree that the mass rate analysis would be interesting and, in fact, this was written at the end of the Conclusions.

We would like to keep this title (also Gettelman et al. 2013, who dealt with mass rates, used a general title “Microphysical process rates and global aerosol-cloud interactions”). Nevertheless, we agree that the reader should understand soon that the paper will focus on number rates, therefore, we made this clear in the Abstract.

### *II) Sublimation*

*Why is sublimation not considered as a sink of ice number in the analysis, particularly after being mentioned in Eq. 1? I think it would be good to find a way to include sublimation in the analysis or at least estimate its impact.*

In the CLOUD submodel, sublimation is taken into account as an IC sink, but it is not dealt as an independent term. Inside the code, sublimation can only affect sedimentation, this is the reason why we wrote that “*SEDI includes also the sublimation of falling ICs*” at L172. The separation between sublimation and sedimentation is not straightforward and we cannot include it in this study.

### *III) Closing the number budget and “numerical tendencies”*

*How close are you to closing the number budget? Are (sources+sinks)\*model timestep = ICNC?*

*Your manuscript offers an often neglected insight into sources of ice, which is rarely seen in publications. However, you do not include “numerical tendencies” in the analysis. I think it would be valuable to show all numerical/unphysical tendencies (correction terms) that significantly perturb the ICNC budget besides the mentioned physical tendencies. An example of such unphysical sink of ice (that you did not mention in the manuscript) is the maximum ICNC correction term. The ice cloud community should become more aware of all such terms and think about ways to avoid imposing such unphysical limits in the models of microphysics. By doing so, the ICNC picture would be complete, and you could close the sources and sink budget. This is in my opinion more important than limiting your analysis to the tendencies with physical meaning only. A strong additional message coming out of your work could therefore be that the very “volatile” ICNC budget is significantly modified by “numerical tendencies”.*

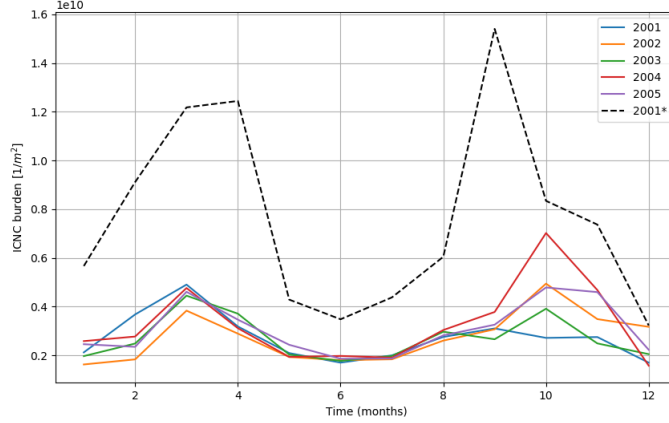


Figure 1: Annual cycles of monthly means of vertically integrated ICNC global means. Continuous lines refer to the REF simulation; the dashed line refers to the test-simulation without the maximum ICNC threshold (NOicncmax).

The number budget cannot be closed in this study because the advective, turbulent, and convective transport tendencies are not taken into account in our analysis (as written at L153). Moreover, in order to close the budget for in-cloud ICNC, the time integration using the Asselin filter should be applied.

What we checked was the validity of the following equality at a given timestep:

$$\sum R_i = (ICNC_{final} - ICNC_{initial})/\delta t$$

where  $R_i$  are all ICNC tendencies detected in CLOUD (both physical and numerical),  $ICNC_{initial}$  is the ICNC input value for CLOUD,  $ICNC_{final}$  is the updated value of ICNC in CLOUD,  $\delta t$  is the model time step.

In order to show, approximately, that the ICNC budget in EMAC is closed, we computed the annual cycles of the vertically integrated ICNC global means (Figure 1 in this document); it is evident that all years show the same behaviour, without any statistical trend.

In the old manuscript, we focused on the physical tendencies (as written at L173-176) and mentioned the existence of the numerical tendencies, providing the example of the maximum correction term, i.e. the threshold  $10^7 \text{ m}^{-3}$  for ICNC. Nevertheless, we agree with the Referee that including the analysis of the numerical tendencies would yield the awareness of the potentially important role of the numerical tendencies in computing ICNC. Therefore, we included this analysis in the revised manuscript.

Additionally, a test-simulation (NOicncmax) was run by removing the condition that ICNC must not exceed  $10^7 \text{ m}^{-3}$ . Figure 1 shows the strong impact of this condition on ICNC, whose values are much higher than ICNC in REF.

Some new text regarding the numerical tendencies and the new test-simulation has been added in the revised manuscript in the Abstract (L6), Introduction (L76-79), Section 2 (with the addition of a new subsection), Section 3, Section 5, and Conclusions.

#### IV) *FREE* term

*I don't think you can physically justify the existence of FREE by simply referring to it as "liquid origin cirrus". The work of Krämer et al., 2016 associates liquid origin cirrus to deep convection (which is DETR in your case) or frontal ascent (e.g. warm conveyor belts). Wernli et al., 2016 shows a peak in liquid origin over the storm track region due to slow frontal ascent. However, in your simulations, FREE is strikingly high over continents and orography. We know wave clouds could be formed by homogeneous freezing of cloud droplets (Heymsfield and Miloshevich, 1993), but that should not matter much in a climatic sense. Homogeneous freezing of cloud droplets is to my understanding of ice cloud formation mechanisms climatically irrelevant outside of deep convective updrafts (and those are taken care of by deep convective scheme and DETR tendency). I would therefore argue that one of the partly unphysical tendencies mentioned in the upper comment is your FREE term. I believe FREE is to a large extent just a temperature correction term that freezes the cloud droplets at temperatures  $< -35^{\circ}\text{C}$ . Ideally, other processes in the model should take care of that and freeze most of the cloud droplets at warmer temperatures. Such terms appear also in other models. Do you believe we should be worried if they represent such a dominant source of ice? Why?*

*How would ICNC look like if you neglected the FREE tendency? Would a short experiment without the FREE source term help understanding its real climatic importance? FREE, as you mention, does not happen very often, but results in huge ICNC. Therefore I would also expect the FREE term to often exceed the maximum ICNC threshold of  $10^7 \text{ m}^{-3}$  and therefore be immediately limited by the "maximum ICNC correction" IC sink. The net climatic effect of such a tendency may therefore be limited. In summary of my lengthy comment, I believe the manuscript would benefit substantially if you better explored the causes of FREE.*

Although FREE is represented in the model simply (like a condition which converts into ICs those cloud droplets that are transported in regions where temperature is below the freezing threshold), its inclusion in cloud microphysics schemes goes back at least to Levkov et al. (1992), as far as we know. According to Krämer et al. 2016, liquid-origin cirrus are formed by water droplets that freeze spontaneously when they reach the homogeneous freezing threshold. This is also the definition of FREE in EMAC, and assigning the meaning of FREE to liquid-origin cirrus is in agreement with Wernli et al. 2016 and Muench and Lohmann (2020). Therefore, we think that it is correct to treat FREE as a microphysical tendency and not a numerical tendency. Moreover, Muench and Lohmann (2020) also considered the freezing of cloud droplets as a source of ICs, although they developed the representation of such process considering its dependence on updraft velocity. More precisely, they analysed the following sources of ICs: homogeneous nucleation (our NCIR), heterogeneous nucleation in cirrus clouds (which is included in our NCIR as well), heterogeneous nucleation in mixed-phase clouds (our NMIX), convective detrainment (our DETR), and droplet freezing (our FREE). The global distribution and the zonal mean of their freezing are similar to our results. We discussed these points in the revised manuscript (in Section 2.2, in the analysis of the results in Section 5, and in Conclusions).

In order to investigate in more depth the role of FREE (as suggested by the Referee), we performed another test-simulation (NOfree) where the tendency FREE is neglected. The description of the new simulation NOfree and its analysis have been added in Section 3 and in the new Section 5.1, respectively. In summary, we found that the tendencies in NOfree remain similar to the ones computed in the REF simulation, but ICNC globally decreases by

one order of magnitude and CDNC instead increase by 10%.

#### *V) Relative importance of specific sources and sinks of ice*

*It is hard to understand the relative importance of specific source and sink processes only by looking at the zonally averaged Fig. 2 and 3. Could you add plots showing the relative importance of each process, i.e. a division of a specific source or sink process with the total source or sink tendency. Would a similar type of plot help in exploring the regional importance of several sources and sinks of ice in the discussion of Fig. 1 and Fig 4?*

*It may be easier to understand the importance of the separate microphysical rates if you would include also figures/information about: a) Probability density function distributions for each microphysical rate, plotted only when the rate has a non-zero value. b) Occurrence frequency of each of the microphysical rates.*

We computed the occurrence of each microphysical process considering non-zero values (new Figure 3 in the manuscript). For an easier comparison between processes, we preferred not to normalize the counts (to get a PDF). Moreover, we computed the relative contributions of the mean tendencies, and we represented them in pie charts. The relative importance was computed for the global means (new Figure 2) and for the regional means (new Figure S3 in the Supplement). We would like to stress the new Table 4 contains also the means and the standard deviations for the two new test-simulations. Since the distributions of the tendencies are described in the new Figure 3, the 1th and 99th percentiles were removed from the Table. The new figures are commented in the new Subsection 5.1 “Global statistics”.

#### *VI) SEDI tendency*

*Why is the vertically integral of SEDI so negative? Shouldn't we think of sedimentation only as a redistribution of ice crystals? Shouldn't the column integrated net SEDI be equal to zero? I know this is not possible due to the inclusion of sublimation of falling ice crystal into the sedimentation tendency. Could you therefore (1) analyse that tendency separately and (2) verify if the net SEDI is now close to be balanced. I don't understand the reasoning you give explaining the disagreement between SEDI+ and SEDI- in lines 245-247. Isn't SEDI- in level X same as SEDI+ in level X-1? (if we take care for the sublimation of falling ice)*

*Moreover the median vertical profiles in Fig. 4 suggest that the vertical integral of sedimentation should be a small values, and not a significantly negative tendency as shown in Fig. 1. The zonally averaged perspective shows SEDI- being more dominant than SEDI+ at all levels of the atmosphere. Why is there such a disagreement between Fig 4 and Figs. 2+3?*

SEDI is a vertical redistribution of ICs (as written at L170). The vertical integration of SEDI in Fig. 1 was not zero because it was (wrongly) computed with monthly means. While using monthly means for the other tendencies is correct because each tendency has only positive or negative sign (and the mean computed with monthly means is equal to the mean computed with original output data), it was a mistake to use monthly means to compute the vertical integration of SEDI. In order to get a vertical integration of SEDI close to zero we have to use instantaneous values, as in Figure 2 (in this document). Nevertheless, SEDI cannot be exactly zero because of the inclusion of IC sublimation (as written at point II), sublimation affects sedimentation) and because SEDI is a net sink close to the ground (at the lowermost model level).

Since sedimentation is not a microphysical process but is a redistribution of existing ICs, we

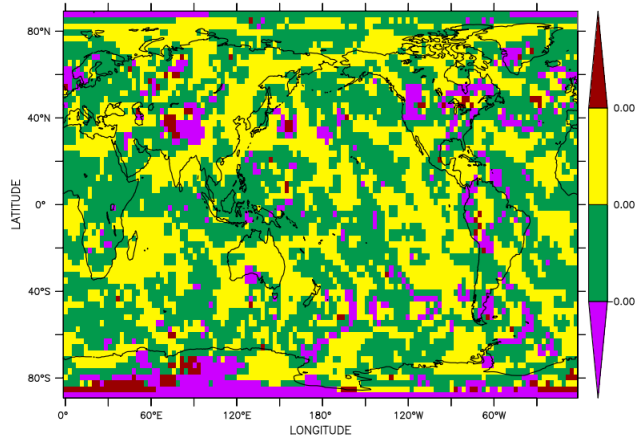


Figure 2: Vertical sum of instantaneous values of SEDI at one model time step (in  $10^5 \text{ m}^{-2} \text{ s}^{-1}$ ).

decided to remove the analysis of SEDI in the revised manuscript.

Regarding question about the vertical profiles in Fig.4, it must be taken into account that they are (median values) computed only where  $\text{ICNC} > 1 \text{ L}^{-1}$ , while the plots in Figs. 2+3 are means computed without any mask, thus, Fig.4 and Figs. 2+3 are not directly comparable. More precisely, in Fig.4, positive and negative values of SEDI cannot be balanced because the statistics is computed for a total number of points which changes at each vertical 20 hPa-bin due to the application of the mask ( $\text{ICNC} > 1 \text{ L}^{-1}$ ) at each bin.

### VII) Summary chart

*You could add a summary chart (maybe a pie chart for sinks and sources of ice or a bar chart) that summarizes the importance of several sources and sink processes. Table 3 is to some extent doing that, but tables are hard to read (and also table 3 is not really giving us a budget perspective). I think that such a visualization (maybe in relative, not absolute terms) would be a nice key figure of the paper.*

Please, see our reply to point V).

### VIII) Effects due to global warming

*Section 4.4.2 is currently very weak and doesn't really provide much of robust novel findings. The only robust feature is the upward shift of ice rates/ICNC. The changes to ICNC, IWC, IWP, source and sink processes cannot be considered robust when comparing only 1 year of data (!). This is confirmed by no significance in zonally averaged plots (I don't consider a 70% significance level adequate).*

*The upward shift in clouds (and therefore sources/sinks of ice) is not novel, so I suggest removing the section and rather focus on digging more into the model to better understand the above mentioned points. If you really want to keep it, you should substantially expand your analysis. A climate change or cloud feedback perspective on the shifts of ice phase with global warming would certainly need some new plots, e.g. changes in ICNC, IWC, IWP, specific and relative humidity, a cloud feedback decomposition (or at least changes in cloud radiative effects assuming an adjustment term to take into account changes in clear sky quan-*

*tities/changes between a CRE and a cloud feedback perspective). Maybe also changes in static stability, radiative heating, etc. Moreover, you did not take advantage of the high frequency output data. How does the ICNC distribution shifts (a) in total (b) in specific temperature ranges? What about IC sources and sinks?*

We thank the Referee for his feedback. We have strengthened the section on global warming by comparing five years of data in the reference period to five years in the warming period and adding new analysis.

## Minor Comments

L4: *How could you compare microphysical process rates with observations? Sadly, I think it's hard to measure the relevant number process rates with the available insitu or remote sensing data. Observations currently lack the evolution perspective, and rather give snapshots of cloud properties.*

We are limited in such an observational comparison, since it is not straightforward to infer the process by which an ice crystal was formed (shape, size, proximity to convection and aerosol source). This additional data is not available at the global scale.

L13: *You could verify whether cloud diabatic heating rates increase in the upper troposphere with the additional model diagnostics.*

We verified this with the new Figure 10, where we do indeed see that the longwave radiative heating associated with ice clouds increases by 0.2-0.3 K per day in the upper atmosphere.

Intro: *A reference mentioning the work by Dietlicher et al., 2019 who showed the cloud volume based on source may be appropriate, although the distinction is not necessarily a process-rate based one. A reference to Gyrspoord et al., 2018 may also be appropriate given their cirrus classification scheme.*

We added the first reference in the Introduction and the second one in the new Section 4 (see next point).

Sec. 4: *I would find it useful if you started the paper by showing the ICNC zonal average and ICNC burden plots (S1 and S2a) and compare that with observations (Sourdeval et al., 2018 and Gryspeerdt et al., 2018). Why does your model overestimate ICNC in the extratropics while simulating too little ICNC in the tropics?*

We included Figures S1, S2a and two new plots for in-cloud ICNC retrieved from satellite products (we used the DARDAR data set) in the new Section 4 “*ICNC model results and evaluation*”. We discussed in the Conclusions that FREE could cause an overestimation of ICNC.

Secs. 2.1-2.2: *Is snow diagnostic? Is it removed from the atmosphere in one timestep? Does it affect radiation or not?*

Snow (precipitation) is fully diagnostic. Vertical advection of snow is not explicitly calculated, and snow reaches the ground in the same time step in which it is formed. Snow, which is not a prognostic variable nor a 3D variable, does not interact with the radiation scheme.

L123: *The convective scheme should detrain some ice also at temperatures warmer than  $-35^{\circ}\text{C}$ . A recent publication by Coopman et al., 2020, for example, shows that the average glaciation temperature of isolated convective clouds over Europe is about  $-21^{\circ}\text{C}$ . That may be worth mentioning in the text as a potential problem of the scheme and reason for low ICNC bias in mixed phase compared to observational data by Sourdeval et al., 2018.*

We thank the referee for the interesting reference; we cited it in Section 4.2.

Sec. 2.3: *Please describe how each of the IC sinks works (not only refer to older publications, given the central role of such processes in your paper). Is there a temperature dependence (particularly for aggregation, accretion, and self collection)? Is there any size dependence?*

We expanded the paragraph “Sinks of ice crystals”, replying to the Referee’s questions.

Sec. 3: *Do you run your global warming simulation in present-day  $\text{CO}_2$  concentrations? If so, do you expect any influence from not changing  $\text{CO}_2$  levels to those expected in year 2080 in the RCP6.0 scenario?*

The  $\text{CO}_2$  emissions in the FUT simulation are taken from the RCP6.0 scenario (see L198 in the manuscript), therefore, the results of FUT already include the influence due to  $\text{CO}_2$  level changes.

L230-233: *“In fact, upper-level gravity wave activity, particularly strong in the tropics, can generate temperature fluctuations responsible for strong nucleation tendencies.”*

*Is this right? Your model resolution is about  $3^{\circ} \times 3^{\circ}$ , which is orders of magnitude larger than the relevant length scales for gravity waves. So the model cannot resolve those directly. Moreover, the model used doesn’t seem to have a parameterization that would add a gravity wave updraft spectrum in to the vertical velocity and in such way represent the influence of gravity waves on ice nucleation. I guess the used TKE-based updraft only gives one vertical velocity value per gridbox, not a distribution. I believe the reason for high ice nucleation rates in the tropical upper troposphere therefore lies in a combination of cold temperature and high relative humidity.*

We removed this sentence and we changed L229-232.

L240: *“On the contrary,  $\text{SEDI}+$  is low at upper levels because the crystals are too small to fall out and at lower levels because the number of ICs is a small.”*

*That doesn’t sound right or I simply don’t understand it. Wouldn’t that be true for  $\text{SEDI}-$  and not  $\text{SEDI}+$ . ICs are small at upper levels, but I don’t know why this would limit the  $\text{SEDI}+$  tendency. I would assume  $\text{SEDI}+$  tendency to be larger in locations where ICNC is large and where IC radius is small. This points rather at the upper troposphere.*

We removed this sentence as we do not consider sedimentation in the revised manuscript.

Sec. 4.3 Fig.4: *Why is detrainment so important over Sahara? Why at such higher altitude? I assume the number of points taken for the Sahara figure is small due to the low amount of ice clouds there. That may be added in the discussion.*

*Another general conclusion of this section could be that a clean (southern) Indian Ocean is very similar to a more polluted N. Atlantic? Moreover, I think many atmospheric scientists would rather call that region as “Southern Ocean”, as in this large project*



*https://www.eol.ucar.edu/field\_projects/socrates , for example. When talking about Indian Ocean we normally think of tropics.*

*I still cannot understand whether FREE is an important source of ice or not. A sensitivity experiment in which FREE source would be turned off could help determining that by looking at changes to ICNC.*

In the new profiles over Sahara, which are obtained with 5-years data (instead of 1-year data) of the new simulations considering bins of 25 hPa (instead of 20 hPa), the DETR profile is not visible anymore. According to Table S1 and the new Figure S3, DETR is more important over Amazon than over Sahara. We added some comments, also regarding the profiles over ocean, in Section 4.3.

The region identified as “IND\_oce” is between the Southern Indian Ocean and the Southern Ocean; we specified in the text that with “IND\_oce” we actually mean a region in the Southern Indian Ocean.

We performed a test-simulation without FREE; please, see our reply to point IV).

L310: *Is DETR really maximal at -35°C? I cannot see that from the Fig. 2. Detrainment tendency should be probably maximized at temperatures closer to -50°C (220 K) in the tropics, if we believe the FAT theory (Hartmann and Larson, 2002).*

We changed this line in the revised manuscript.

Sec. 4.4.2: *It is hard to understand whether we see only a shift or some change in ice rates. A temperature vertical axis would therefore be more appropriate for Fig 5.*

For consistency with the other zonal mean plots, we have chosen to keep the pressure level coordinate for this figure.

L313-320: *You mention the ICNC increase in the upper troposphere. Isn't this only a shift due to the expansion of troposphere? If IC radius decreases and if this change is important, you may want to show it in a separate plot.*

We see both an upward shift with the changing atmospheric temperature structure (deepening troposphere as said by the Referee) as well as an increase in the ICNC tendency magnitudes. The colorbar in Figure 5 is symmetric and we see larger magnitude increases than decreases. The IC radius is unfortunately not a default output of these simulations.

L318: *Isn't an increase in cloud persistence in contrast with your comment on decreased upper tropospheric anvil clouds due to increased static stability? I thought the high cloud fraction decreases with warming?*

Yes, we thank the Referee for pointing this out. We have clarified that such a mechanism would counterbalance those associated with increased static stability. Since we see large decreases in upper-level cloud fraction, our results do not support such a “decreased-fall-speed” mechanism.

L315: *Why do you think the LW atmospheric heating is associated with the cloud base temperature? Are you talking about heating within the atmosphere? Or at the top-of-the atmosphere (TOA) radiative effects? I don't think the cloud base temperature matters for the TOA LW effects. Deep convective clouds have a large LW CRE, despite having a very low cloud base (with high temperatures). Maybe some of Mark Zelinka's numerous*

*publications on the topic may help.*

We removed this comment and presented the atmospheric longwave cloud radiative heating rates in the new Figure 10.

L315: *Also, you talk about the additional upper tropospheric warming due to climate change but never explain why should we care if the upper troposphere is slightly warmer? (compared to the arguably more important or at least more studied influence of changes in high clouds on the TOA radiative budget and climate sensitivity).*

We noted that an increase in atmospheric longwave heating from larger ICNCs will stabilise the atmospheric column and suppress deep convection.

L315-316: *I think the sentence “thicker cirrus...” is incorrect. Why only thick cirrus? Also, most cirrus aren’t optically very thick.*

This sentence has now been removed.

L319-320: *I am not sure if the interpretation of the result of Sanderson et al., 2008 is correct, so it may need to be rewritten. Sanderson et al., 2008 found the IC fall speed to be important in modulating the mainly LW cloud feedback (and hence climate sensitivity) not because the IC fall speed would change between the present day and global warming simulation (IC fall speed is not calculated interactively in their simulations, given the use of a tuning parameter). However, a smaller ice fall speed leads to more high clouds. That in turn leads to a larger LW altitude (positive) cloud feedback, which is the dominant high cloud feedback. On the other hand, a smaller present-day cloud fraction due to large ice fall speed, leads to less high clouds and a smaller high cloud feedback and smaller climate sensitivity.*

We thank the Referee for drawing our attention to the details of the Sanderson et al. study. As noted above, we modified the discussion of such a “decreased-fall-speed” mechanism and removed the reference to Sanderson et al 2008. We agree that the smaller ice fall speed would lead to larger high-cloud fraction and a LW cloud feedback. Since we see instead decreased high-cloud fraction, such a mechanism is not dominant in our simulations.

Sec. 4.4.2: *As you talk about ice clouds and not only cirrus, you may want to also explore/mention the cloud phase negative optical feedback due to global warming (Tan et al., 2016, maybe also Bodas-Salcedo 2018 and 2019, Lohmann and Neubauer, 2018).*

We appreciate this suggestion but consider it outside the scope of this work. We would need to dedicate much more space and analysis to looking at shifts in overall cloud water and cloud water tendencies as well.

Concl: *It may be appropriate to think a bit more about some of the questions I listed below and include some of that in the discussion: What did you learn about the model by exposing the number tendencies that you couldn’t by simply taking the ICNC fields? Is there something that we should be worried about? Why? What is causing it? What are the potential weaknesses of the study? How does this compare to other work (if any exists – maybe for mass rates)?*

We enlarged and strengthened the Conclusions with additional discussion about the new analysis and the questions raised by the Referee.

# Authors' reply to Referee #2

## Major Comments

*(1) The model result uncertainty could be very large from a few aspects.*

*(1.1) The model grid spacing is very coarse (300 km) and the output time frequency is very sparse (every 5 hours). Many times, the cloud lifetime can be even less than 10 hours, then the sampling cannot be representative with every 5-hour time frequency. I'd suggest look at the sensitivity to model resolution (such as 100 km) and output time frequency (hourly) to meet the goal of quantification.*

We agree with the observations raised by the Referee. It would be interesting to perform sensitivity runs and investigate the influence of spatial and temporal resolutions on the tendencies. However, running new simulations at various resolutions with hourly output frequency would require much time, and new analysis should be performed. This is not the objective of this paper and could be addressed as an independent study. We mentioned at the end of the Conclusions that this can be an interesting future study.

*(1.2) Need to do ensemble runs for quantification.*

Also in this case, running ensemble experiments would require much time. Nevertheless, in the revised manuscript, the simulations were run for five years (instead of one year) so the analysis of the tendencies is now more robust.

*(1.3) Need to discuss that the results might be changed with different models or different physical parameterizations such as cumulus or microphysics parameterizations.*

In this regard, we added some new lines at the end of the Subsection 4.4.1, where we already discussed the sensitivity of the results to microphysics parameterization changes, and also in the Conclusions.

*(2) For the sink of ice crystal, sublimation should be considered.*

Unfortunately, as replied to Referee #1 point II), the sublimation term is combined with SEDI; the separation between sublimation and sedimentation is not straightforward, and we cannot estimate the sublimation impact individually.

*(3) Result section: I feel a little surprised that the authors started the discussion of results for the source and sink of ice directly. It would be nice to understand the overall model performances in simulating radiation, clouds and precipitation first. Then get to the analysis of ice crystal number concentrations and its budget.*

We added a new section (4 “Model results and evaluation of ICNC”) in the revised manuscript to evaluate the model ICNC against satellite ICNC retrievals before starting with the analysis of the tendencies.

The understanding of the overall model performance in simulating radiation, clouds and precipitation goes beyond the scope of this paper. The EMAC model is continuously developed, tested, and evaluated (against observations and other model results). The EMAC model and all its improvements are well documented in papers of the Special Issue “The Modular Earth Submodel System” of Copernicus and in the MESSy Consortium Website

(<https://www.messy-interface.org>). Section 2.1 provides the standard description of EMAC; L94-95 cites some of the studies which deal with the model performance in simulating different physical quantities (e.g. aerosol burdens, cloud cover, radiation, cloud radiative effects...).

*(4) Since one of the purposes of the study is to test the sensitivity to two other nucleation parameterizations, then some description about the two default and two tested schemes is needed, particularly about how different they are in terms of representing ice formation such as temperature dependent, supersaturation dependent, and aerosol dependent.*

*If aerosol dependent, then what aerosols are considered? Why did you replace the immersion freezing scheme with a contact freezing scheme? Shouldn't they be considered together?*

The differences between the ice nucleation schemes in cirrus regime and mixed-phase regime are detailed in Bacer et al. 2018 (in Sections 2.2., 2.3.1, and Figure 1). We added some information regarding the schemes and also the reference. We specified at L138 that the parameterizations for heterogeneous nucleation are aerosol dependent. The ice nucleation parameterizations working in the mixed-phase regime are listed at L135-138: immersion freezing is not replaced with contact freezing; contact nucleation is always considered via LD06; immersion nucleation can be simulated either via LD06 or P13 (which also simulates deposition nucleation). We made L135-138 clearer.

## Minor Comments

1. *Calling everything below -35 deg C as "cirrus clouds" is not accurate. I would suggest change to "pure ice clouds".*

According to the definitions provided, for example, by Krämer et al. 2016 and Heymsfield et al. 2017, and the terminology used in most of the literature, we consider "cirrus clouds" (i.e. clouds purely composed of ice crystals) equivalent to "pure ice clouds", and we would like to keep this terminology in the manuscript.

2. *For the convective detrainment, does the model treat the detrainment at the levels with  $T > -35$  deg C? If not, is there a reason? Theoretically convective detrainment of droplet and ice can occur from middle to top troposphere.*

Convective detrainment can occur also at  $T > -35^\circ\text{C}$ : the cloud condensate at  $T < -35^\circ\text{C}$  is considered in the ice phase (and it is a source of ICs), while the cloud condensate at  $T > -35^\circ\text{C}$  is considered in the liquid phase (and it is a source of cloud droplets). This is explained at L121-122.

3. *Line 210-215, does FREE include the droplet freezing in convective parameterization?*

FREE does not include ice crystals formed in convective parameterizations. FREE is an independent term defined in the CLOUD submodel (convection is simulated by another submodel, CONVECT), and it includes the ICs formed from liquid water droplets that are transported in regions where temperature is  $< -35^\circ\text{C}$ , as written at L163.

4. *Section 4.2, how to reconcile that DETR is much larger than NCIR in zonal mean (Fig. 2) but smaller than it in global spatial distribution (Fig. 1)?*

We are not sure what the Referee means here, as both Figure 1 and Figure 2 show that DETR is generally higher than NCIR, so the Figures are in agreement.

5. *Line 284-286, I am confused by this sentence. Earlier it is said LD06 is a contact freezing scheme which is for heterogenous freezing. Here you said LD06 parameterizes only homogeneous nucleation. Also P13 should be an immersion freezing scheme which should be much more efficient than the contact freezing LD06, but the results in section 4.4.1 did not even mention the differences they can make.*

We thank the Referee for noticing that there is indeed an inconsistency at L285; we replaced “LD06” with “KL02”.

Since NCIR and NMIX are defined as the rates of new ICs in the cirrus regime and new ICs in the mixed-phase regime, it is not possible to discern the contributions from contact and immersion freezing. However, during some previous tests, we found that immersion nucleation simulated with LD06 produces more ICs than immersion-condensation and deposition nucleation using P13. This is in agreement with Phillips et al. 2008, who compared their empirical parameterization (which is the previous version of P13) with other parameterizations including LD06.

## References

- [1] Bacer, S., Sullivan, S. C., Karydis, V. A., Barahona, D., Krämer, M., Nenes, A., Tost, H., Tsimpidi, A. P., Lelieveld, J., and Pozzer, A.: Implementation of a comprehensive ice crystal formation parameterization for cirrus and mixed-phase clouds in the EMAC model (based on MESSy 2.53), *Geoscientific Model Development*, 11, 4021–4041, 2018.
- [2] Heymsfield, A. J., Krämer, M., Luebke, A., Brown, P., Cziczo, D. J., Franklin, C., Lawson, P., Lohmann, U., McFarquhar, G., Ulanowski, Z., and Van Tricht, K.: Cirrus Clouds, *Meteorological Monographs*, 58, 2.1–2.26, 2017.
- [3] Krämer, M., Rolf, C., Luebke, A., Afchine, A., Spelten, N., Costa, A., Meyer, J., Zöger, M., Smith, J., Herman, R. L., Buchholz, B., Ebert, V., Baumgardner, D., Borrmann, S., Klingebiel, M., and Avallone, L.: A microphysics guide to cirrus clouds Part 1: Cirrus types, *Atmospheric Chemistry and Physics*, 16, 3463–3483, 2016.
- [4] Muench, S. and Lohmann, U.: Developing a cloud scheme with prognostic cloud fraction and two moment microphysics for ECHAM-HAM, *Journal of Advances in Modeling Earth Systems*, 12, 2020.
- [5] Sourdeval, O., Gryspeerdt, E., Krämer, M., Goren, T., Delanoë, J., Afchine, A., Hemmer, F., and Quaas, J.: Ice crystal number concentration estimates from lidar–radar satellite remote sensing – Part 1: Method and evaluation, *Atmos. Chem. Phys.*, 18, 14327–14350, 2018
- [6] Phillips, V. T. J., DeMott, P. J., and Andronache, C.: An Empirical Parameterization of Heterogeneous Ice Nucleation for Multiple Chemical Species of Aerosol, *Journal of the Atmospheric Sciences*, 65, 2757–2783, 2008.

# Cold cloud microphysical process rates in a global chemistry-climate model

Sara Bacer<sup>1,\*</sup>, Sylvia C. Sullivan<sup>2</sup>, Odran Sourdeval<sup>3</sup>, Holger Tost<sup>4</sup>, Jos Lelieveld<sup>1,5</sup>, and Andrea Pozzer<sup>1</sup>

<sup>1</sup>Atmospheric Chemistry Department, Max Planck Institute for Chemistry, Mainz, Germany

<sup>2</sup>Institute of Meteorology and Climate Research, Karlsruhe Institute of Technology, Karlsruhe, Germany

<sup>3</sup>Laboratoire d'Optique Atmosphérique, Université de Lille, CNRS, Lille, France

<sup>4</sup>Institute for Atmospheric Physics, Johannes Gutenberg University Mainz, Mainz, Germany

<sup>5</sup>Climate and Atmosphere Research Center, The Cyprus Institute, Nicosia, Cyprus

\*now at: LEGI, Université Grenoble Alpes, CNRS, Grenoble INP, Grenoble, France

**Correspondence:** Sara Bacer (sara.bacer@univ-grenoble-alpes.fr)

**Abstract.** Microphysical processes in cold clouds which act as sources or sinks of hydrometeors below 0°C control the ice crystal number concentrations (ICNCs) and in turn the cloud radiative effects. Estimating the relative importance of the cold cloud microphysical process rates is of fundamental importance to underpin the development of cloud parameterizations for weather, atmospheric chemistry and climate models and compare the output with observations at different temporal resolutions.

5 This study quantifies and investigates the ICNC rates of cold cloud microphysical process-rates-processes by means of the chemistry-climate model EMAC and defines the hierarchy of sources and sinks of ice crystals. ~~The analysis~~ Both microphysical process rates, such as ice nucleation, aggregation, and secondary ice production, and unphysical correction terms are presented. Model ICNCs are also compared against a satellite climatology. We found that model ICNCs are in overall agreement with satellite observations, although the values around high mountains are overestimated. The analysis of ice crystal rates is carried out both at global and at regional scales. We found that globally the freezing of cloud droplets ~~,along-with-and~~ convective detrainment over tropical land masses ~~,are~~ are the dominant sources of ice crystals, while aggregation and accretion act as the largest sinks. In general, all processes are characterised by highly skewed ~~distribution~~ distributions. Moreover, the influence of (a) different ice nucleation parameterizations and (b) a future global warming scenario on the rates has been analysed in two sensitivity studies. In the first, we found that the application of different parameterizations for ice nucleation ~~changed-only~~ slightly-changes the hierarchy of ice crystal sources only slightly. In the second, all microphysical processes ~~followed~~ follow an upward shift ~~(in-altitude-)~~ in altitude and an increase by up to 10% in the upper troposphere towards the end of the 21st century. ~~This increase could have important feedbacks, such as leading to enhanced longwave warming of the uppermost atmosphere.~~

15

## 1 Introduction

Clouds play a central role in the global energy budget interacting with shortwave solar and longwave terrestrial radiation. Their radiative properties (cloud albedo and emissivity) depend on microphysical and optical characteristics, such as temperature, size distribution and shape of cloud particles, and the phase of water. Despite ~~the great relevance~~ their important role in the

20

Earth System, the understanding of clouds is still challenging and affected by large uncertainties (IPCC, 2013). The numerical representation of clouds must contend with the limited understanding of the fundamental details of microphysical processes as well as the fact that cloud processes span several order of magnitudes (from nanometres to thousands of kilometres). Hence, modelling of clouds remains a weak point in all atmospheric models, regardless of their resolution, and has been recognised as one of the dominant sources of uncertainty in climate studies (IPCC, 2013; Seinfeld et al., 2016).

Modelling the microphysics of cold clouds, which form at temperatures lower than  $0^{\circ}\text{C}$  and involve ice crystals (ICs), is more challenging than that of warm clouds because of the additional complexity of ice processes (Cantrell and Heymsfield, 2005; Kanji et al., 2017; Heymsfield et al., 2017; Korolev et al., 2017; Dietlicher et al., 2019). Some examples of these processes are include heterogeneous ice nucleation, which depends on particular aerosols and occurs via different modes; the secondary production mechanisms of ice crystals, which involve collisions of ICs; the competition for water vapour among different ice particles; and the thermodynamic instabilities when both liquid and ice phases coexist. Additionally, the variety of possible ice crystal shapes from dendrites to needles also determines the radiative impact of cold clouds and complicates their representation in large-scale models (Lawson et al., 2019). Cold clouds are classified as cirrus clouds when they purely consist of ICs at temperatures generally lower than  $-35^{\circ}\text{C}$ , and as mixed-phase clouds when they include both ICs and supercooled liquid cloud droplets between  $-35^{\circ}\text{C}$  and  $0^{\circ}\text{C}$ . Cirrus clouds strongly impact the transport of water vapour entering the stratosphere, which in turn has a strong effect on radiation and ozone chemistry (Jensen et al., 2013), and produce a positive net radiative effect at the top of the atmosphere (TOA) (Chen et al., 2000; Hong et al., 2016; Matus and L'Ecuyer, 2017); on the other hand, mixed-phase clouds exert a negative net radiative effect at the TOA, although the estimates of their radiative effect are complicated by the coexistence of both ice and liquid cloud phases (Chen et al., 2000; Hong et al., 2016; Matus and L'Ecuyer, 2017).

Several categories of microphysical processes have been identified in cold clouds (Pruppacher and Klett, 1997) that. These can be broadly classified as formation, growth, and loss processes of ice crystals. New ICs are formed thermodynamically via two ice nucleation mechanisms, depending on environmental conditions (e.g. temperature, supersaturation, and vertical air motions) and aerosol populations (i.e. aerosol number concentrations and physicochemical characteristics, such as composition, shape, and surface tension) (Pruppacher and Klett, 1997; Kanji et al., 2017; Heymsfield et al., 2017). Homogeneous ice nucleation occurs at low temperatures (below  $-35^{\circ}\text{C}$ ) and high ice saturation ratios (140% – 160%) via the freezing of supercooled liquid cloud droplets. Heterogeneous ice nucleation takes place at warmer but still subzero temperatures and lower ice supersaturation thanks to the presence of particular atmospheric aerosols, called ice nucleating particles (INPs). It occurs via four different mechanisms, or ice nucleation modes: contact nucleation, condensation nucleation, immersion, and deposition nucleation modes. ICs can also be produced from the multiplication of pre-existing ice crystals, via the so-called secondary ice production (or ice multiplication). Several mechanisms of secondary ice production have been identified. In rime splintering (or the Hallett-Mossop process), small ice crystals (or splinters) are ejected after the capture of supercooled droplets by large ice particles (e.g. graupels) between  $-3^{\circ}\text{C}$  and  $-8^{\circ}\text{C}$ . In collisional break-up (or collisional fragmentation), the disintegration of fragile, slower-falling dendritic crystals which that collide with dense graupel particles produces smaller ice particles. Droplet shattering involves the freezing of large cloud droplets and their subsequent shattering. Sublimation fragmentation occurs when



ice particles break from parent ice particles after the sublimation of “ice bridges” at ice subsaturated conditions. Additionally, ICs can be generated in the vicinity of deep convective clouds by their lateral outflow or detrainment.

A variety of ice growth mechanisms also exist. In conditions of ice supersaturation, ICs grow by diffusion as ambient water vapour deposits. When both ice and liquid phases coexist, the water vapour is generated by evaporating water droplets because of the difference between the saturation vapour pressure over ice and over water (Wegener-Bergeron-Findeisen – WBF mechanism). The collision-coalescence (or collection) between ICs and other hydrometeors is another growth mechanism which occurs in several ways (Rogers and Yau, 1989; Khain and Pinsky, 2018): self-collection consists of the collision-coalescence between ICs and the production of ice crystals with larger size; aggregation occurs when the colliding ICs clump together to form an aggregated snowflake; accretion indicates the collection between ice crystals and snowflakes; and riming refers to the collision of ICs with supercooled liquid droplets which freeze upon contact. Melting and sublimation are other sinks of ice crystals when temperatures are higher than 0°C and there is ice subsaturation, respectively.

~~Ice water content, the particle size distribution, and cloud optical depth all depend on ice~~ Ice crystal number concentration (ICNC) ~~, and their improved representation in models allows for more realistic estimates~~ influences microphysical and optical properties of cold clouds, so an accurate ICNC estimate allows for a more realistic representation of the cloud radiative effects. ~~For this reason, many~~ Many efforts have been made to parameterize all relevant microphysical processes which affect ICNC (e.g. Kärcher and Lohmann, 2002a; Barahona and Nenes, 2008; Phillips et al., 2007; DeMott et al., 2010; Hallett and Mossop, 1974) and to further improve the existing parameterizations (e.g. Kärcher and Lohmann, 2002b; Barahona and Nenes, 2009; Phillips et al., 2013; DeMott et al., 2016; Sullivan et al., 2018b, a). The parameterizations have been implemented in general circulation models (GCMs) which may use a two-moment cloud microphysics scheme (e.g. Liu et al., 2012; Barahona et al., 2014; Kuebbeler et al., 2014; Bacer et al., 2018) to advance the simulation of cloud phase partitioning and cloud-radiation feedbacks.

It is of crucial importance to know the hierarchy of sources and sinks of ICs under different thermodynamic conditions and over different time scales. In fact, knowing these relative contributions facilitates the comparison of simulation output with observations across temporal resolutions and the development of scale-aware microphysics schemes. Gettelman et al. (2013) analysed the rates of the processes affecting precipitation ~~(e.g. condensation, accretion, autoconversion, sedimentation of liquid droplets, WBF, homogeneous nucleation, and heterogeneous nucleation)~~ in the CAM5 model. ~~To~~ Muench and Lohmann (2020) presented some information about ice crystal sources in the ECHAM-HAM model. Nevertheless, to the best of our knowledge, a detailed quantitative analysis of all the microphysical processes affecting ICNC has not yet been performed. Moreover, ICNC in GCMs is also affected by unphysical correction terms (or numerical rates) that are usually neglected in scientific investigations. Therefore, this study aims to estimate and investigate carefully the rates of the microphysical processes and the unphysical corrections which act as sources or sinks of ice crystals and control ICNC in cold clouds for the first time. The analysis is carried out both at global and at regional scales. We also discuss how the rates will change under a global warming scenario towards the end of the century. For this study, the numerical simulations have been performed with the global ECHAM/MESSy Atmospheric Chemistry (EMAC) model.

The paper is organised as follows. We first describe the EMAC model and the numerical representation of the ~~ice-microphysical processes-ICNC rates~~ inside the model (Section 2). Then, the simulations are detailed (Section 3) and ~~model-output-the ICNC output data are compared with ICNC satellite estimations (Section 4). The model results for microphysical and numerical rates are presented~~ at both the global and the regional scale ~~is presented (Section 5). We (Section 5): we~~ also show the robustness of these results to the ice nucleation parameterization, as well as their sensitivity to global warming with an RCP6.0 simulation. ~~We finish with our Conclusions~~ Finally, we present our conclusions (Section 6).

## 2 Ice microphysical processes in EMAC

### 2.1 The EMAC model

The EMAC model is a global chemistry-climate model which describes tropospheric and middle-atmospheric processes and their interactions with ocean, land, and human influences. EMAC combines the 5th generation European Centre Hamburg GCM (ECHAM5, Roeckner et al., 2006), the core of the atmospheric dynamics computations, with the Modular Earth Submodel System (MESSy, Jöckel et al., 2010), which includes a variety of submodels describing physical, dynamical, and chemical processes. For the present study we used ECHAM5 version 5.3.02 and MESSy version 2.53.

The EMAC model has been extensively used and evaluated against in-situ, aircraft, and satellite observations of, for example, aerosol optical depth, acid deposition, meteorological parameters, cloud radiative effects (e.g. Pozzer et al., 2012, 2015; Karydis et al., 2016; Tsimpidi et al., 2016; Klingmüller et al., 2018; Bacer et al., 2018). EMAC computes gas-phase species online through the Module Efficiently Calculating the Chemistry of the Atmosphere (MECCA) submodel (Sander et al., 2011) and provides a comprehensive treatment of chemical processes and dynamical feedbacks through radiation (Dietmüller et al., 2016). Aerosol microphysics and gas/aerosol partitioning are calculated by the Global Modal-aerosol eXtension (GMXe) submodel (Pringle et al., 2010), a two-moment aerosol module which predicts the number concentration and the mass mixing ratio of the aerosol modes. The aerosol size distribution is described by seven lognormal modes: four hydrophilic modes, which cover the aerosol size spectrum of nucleation, Aitken, accumulation, and coarse particles, and three hydrophobic modes, which have the same size range except for the nucleation particles. The aerosol composition within each mode is uniform (internally mixed) but it varies among the modes (externally mixed). The ONEMIS and OFFEMIS submodels describe the online and offline emissions, respectively, of tracers and aerosols, while the TNUDGE submodel performs the tracer nudging towards observations (Kerkweg et al., 2006b). Physical loss processes, like dry deposition, wet deposition, and sedimentation of aerosols and trace gases, are explicitly considered by the submodels DDEP, SEDI, and SCAV (Kerkweg et al., 2006a; Tost et al., 2006a). The RAD submodel (Dietmüller et al., 2016) calculates the radiative transfer taking into account cloud cover, optical properties of clouds and aerosols, mixing ratios of water vapour and radiatively active species, and orbital parameters. Convective and large-scale clouds are parameterized via two different submodels, the CONVECT submodel (Tost et al., 2006b) and the CLOUD submodel (Roeckner et al., 2004), as described in the next Subsection.

In EMAC, a single updraft velocity ( $w$ ) is used for the whole grid cell, although the vertical velocity varies strongly in reality within the dimensions of a grid box (e.g. Guo et al., 2008). This is a simplification which is commonly used by GCMs. The

subgrid-scale variability of vertical velocity ( $w_{sub}$ ) is introduced by a turbulent component which depends on the subgrid-scale  
125 turbulent kinetic energy (TKE) described by Brinkop and Roeckner (1995). Thus, the vertical velocity is given by the sum of  
the grid mean vertical velocity ( $\overline{w}$ ) and the turbulent contribution:  $w = \overline{w} + 0.7\sqrt{TKE}$  (Lohmann and Kärcher, 2002).

## 2.2 Numerical representation of clouds

Convective cloud microphysics in EMAC is solely based on temperature and ~~updraught~~updraft strength and does not take into  
account the aerosol influence on cloud droplet and ice crystal formation. To simulate convective clouds, the CONVECT sub-  
130 model includes multiple parameterizations which address the influence of the convective activity on the larger scale circulation  
~~-.The by adding the~~ detrained water vapour ~~is-added~~ to the large-scale water vapour field. The detrained cloud condensate is  
used as a source term for the cloud condensate treated by the CLOUD submodel and ~~it~~ is considered in the liquid or ice phase  
depending on its temperature (if ~~the~~ temperature is lower than  $-35^{\circ}\text{C}$  the phase is ice, otherwise it is liquid). In this work, the  
scheme of Tiedtke (1989) with modifications by Nordeng (1994) has been used.

135 The CLOUD submodel describes physical and microphysical processes in large-scale stratiform clouds. It uses a double-  
moment cloud microphysics scheme for cloud droplets and ice crystals (Lohmann et al., 1999; Lohmann and Kärcher, 2002;  
Lohmann et al., 2007) and solves the prognostic equations for specific humidity, liquid cloud mixing ratio, ice cloud mixing  
ratio, cloud droplet number concentration (CDNC), and ICNC. Cloud droplet formation is computed by an advanced physically  
based parameterization (Kumar et al., 2011; Karydis et al., 2011) ~~which-that~~ merges two theories: the  $\kappa$ -Köhler theory (Petters  
140 and Kreidenweis, 2007), which governs the activation of soluble aerosols, and the Frenkel-Halsey-Hill adsorption activation  
theory (Kumar et al., 2009), which describes the droplet activation due to water adsorption onto insoluble aerosols (e.g. min-  
eral dust). This parameterisation is applied to the aerosols that consist of an insoluble core with soluble coating, while soluble  
aerosols follow the  $\kappa$ -Köhler theory (Karydis et al., 2017). In the cirrus regime, ~~the~~ ice crystals can form either via homoge-  
neous nucleation, using the parameterization of Kärcher and Lohmann (2002b, KL02), or via homogeneous and heterogeneous  
145 nucleation using the parameterization of Barahona and Nenes (2009, BN09), which takes into account the competition for  
the available water vapour between the two ice nucleation mechanisms and among the pre-existing ice crystals (Bacer et al.,  
2018). In the mixed-phase regime, contact nucleation is simulated according to Lohmann and Diehl (2006, LD06). Immersion  
nucleation can be parameterized either via LD06 or via the empirical parameterization of Phillips et al. (2013, P13), which  
can also simulate deposition nucleation. Both LD06 and P13 are aerosol dependent. In this study, LD06 considers insoluble  
150 mineral dust for contact nucleation and soluble dust and black carbon for immersion nucleation, while P13 takes into account  
insoluble dust and black carbon, and glassy organics for immersion and deposition nucleation. (For a detailed comparison of  
the ice nucleation parameterizations BN09, KL02, LD06, and P13 we refer to Bacer et al. (2018).) Cloud cover is computed  
diagnostically with the scheme of Sundqvist et al. (1989), based on the grid-mean relative humidity. Other microphysical pro-  
cesses, like phase transitions, autoconversion, aggregation, accretion, evaporation of rain, melting of snow, ~~sedimentation-of~~  
155 ~~cloud-ice~~, are also taken into account by the CLOUD submodel.

<u>Tendency</u>	<u>Description</u>	<u>Temperature</u>
<u>DETR</u>	<u>Convective detrainment</u>	<u><math>T &lt; -35^{\circ}\text{C}</math></u>
<u>NCIR</u>	<u>Ice nucleation in the cirrus regime</u>	<u><math>T &lt; -35^{\circ}\text{C}</math></u>
<u>FREE</u>	<u>Instantaneous freezing</u>	<u><math>T &lt; -35^{\circ}\text{C}</math></u>
<u>NMIX</u>	<u>Ice nucleation in the mixed-phase regime</u>	<u><math>-35^{\circ}\text{C} &lt; T &lt; 0^{\circ}\text{C}</math></u>
<u>SECP</u>	<u>Secondary ice production</u>	<u><math>-8^{\circ}\text{C} &lt; T &lt; -3^{\circ}\text{C}</math></u>
<u>MELT</u>	<u>Melting</u>	<u><math>T &gt; 0^{\circ}\text{C}</math></u>
<u>SELF</u>	<u>Self-collection</u>	<u><math>T &lt; 0^{\circ}\text{C}</math></u>
<u>AGGR</u>	<u>Aggregation</u>	<u><math>T &lt; 0^{\circ}\text{C}</math></u>
<u>ACCR</u>	<u>Accretion</u>	<u><math>T &lt; 0^{\circ}\text{C}</math></u>

**Table 1.** ICNC tendencies of the microphysical processes defined in the CLOUD submodel. Sources of ICs are in the highest block, sinks of ICs are in the lowest block. The first column contains the abbreviations associated with each tendency; the second column describes the microphysical processes associated with each tendency; the third column specifies the temperature range in which the processes occur.

## 2.3 Ice-microphysical-processes ICNC tendencies

### 2.3.1 Microphysical tendencies

According to Lohmann (2002) and Roeckner et al. (2004), the evolution of ICNC (i.e. rate or tendency of ICNC) is described by the following prognostic equation:

$$\frac{\partial \text{ICNC}}{\partial t} = R_{\text{transp}} + R_{\text{sed}} + R_{\text{ncir}} + R_{\text{nmix}} + R_{\text{secp}} - (R_{\text{self}} + R_{\text{aggr}} + R_{\text{accr}} + R_{\text{melt}} + R_{\text{subl}}) \quad (1)$$

where the  $R$ -terms (in  $\text{m}^{-3}\text{s}^{-1}$ ) are the ICNC tendencies due to specific ~~(micro)physical~~ physical or microphysical processes: advective, turbulent, and convective transport ( $R_{\text{transp}}$ ), sedimentation ( $R_{\text{sed}}$ ), ice nucleation in the cirrus regime ( $R_{\text{ncir}}$ ), ice nucleation in the mixed-phase regime ( $R_{\text{nmix}}$ ), secondary ice production ( $R_{\text{secp}}$ ), self-collection ( $R_{\text{self}}$ ), aggregation ( $R_{\text{aggr}}$ ), accretion ( $R_{\text{accr}}$ ), melting ( $R_{\text{melt}}$ ), and sublimation ( $R_{\text{subl}}$ ) of ice crystals. Transport as well as sedimentation of ICs are computed for the grid-box volume ( $\overline{\text{ICNC}}$ ), while the other terms are in-cloud processes ( $\text{ICNC}_{\text{in-cloud}}$ ). The latter ones are related to the grid-mean values via the fractional cloud cover ( $f_C$ ):  $\text{ICNC}_{\text{in-cloud}} = \overline{\text{ICNC}}/f_C$ . Among the processes in equation (1), advective, turbulent, and convective transport and sedimentation (which vertically redistributes the ICs and is formally treated like vertical advection) are physical processes solved by the model, while all others are microphysical processes computed with different parameterizations.

In this work, we decompose the microphysical sources and sinks of ICs in the CLOUD submodel (Table 1), i.e. all  $R$ -terms except  $R_{\text{sed}}$  and  $R_{\text{transp}}$ . ~~(More information can be found in the cited works and references therein.)~~ It must be mentioned that sublimation of falling ICs that encounter an ice subsaturated region has not been analysed in this work as it is included in  $R_{\text{sed}}$ .

**Sources of ice crystals.** The number of new ICs originating from convective detrainment (DETR) is estimated from the detrained cloud condensate in the ice phase (i.e. when ~~temperatures are lower than  $-35^{\circ}\text{C}$~~  temperature is lower than  $-35^{\circ}\text{C}$ , see

Subsection 2.2) by assuming a temperature dependent IC radius. DETR is included in the transport term of equation (1) (Roeckner et al., 2004), but it will be studied here as an independent source of ICs defined within the CLOUD submodel. As described in Subsection 2.2, ice crystal formation in the cirrus regime (NCIR) is simulated by via the ice nucleation parameterizations BN09 or KL02. ~~The new ICs in~~ Moreover, supercooled cloud droplets freeze instantaneously (FREE), i.e. they glaciate in one time step, when they are transported to regions where temperature is below  $-35^{\circ}\text{C}$  (like in Levkov et al., 1992). In the mixed-phase regime, the number of new ICs formed via heterogeneous nucleation (NMIX) are-is the sum of the ice crystals originated from contact, immersion/condensation, and deposition nucleation modes, i.e. the results of the heterogeneous nucleation parameterizations LD06 and/or P13 applied in this regime. Secondary ice production (SECP) occurs via the Hallet-Mossop process between  $-3^{\circ}\text{C}$  and  $-8^{\circ}\text{C}$  as described in Levkov et al. (1992). ~~Another source of ICs is the instantaneous freezing of supercooled cloud droplets (FREE); when temperatures are below~~ NCIR represents in-situ cirrus clouds, those forming at temperatures colder than  $-35^{\circ}\text{C}$  ~~, the cloud droplets which did not freeze through ice nucleation become ICs. FREE represents (in a numerical way) the so-called via heterogeneous or homogeneous ice nucleation of solution droplets. FREE represents liquid-origin cirrus, i.e. cirrus clouds formed by ICs originated via homogeneous nucleation at temperatures near the homogeneous nucleation threshold which are then lifted in the cirrus regime. Instead, NCIR represents the in-situ cirrus, i.e. cirrus clouds which form directly at temperatures colder than whose ICs are generated by the advection of already-formed water cloud droplets below  $-35^{\circ}\text{C}$  (Krämer et al., 2016); this process is particularly active in regions with mesoscale convective activity and warm conveyor belts (Krämer et al., 2016). Also immersion and contact nucleation contribute to form liquid-origin cirrus (Wernli et al., 2016), but they are considered in NMIX here.~~

**Sinks of ice crystals.** ~~Self-collection~~ In general, self-collection (SELF), aggregation (AGGR), and accretion (ACCR) of ice crystals follow Lin et al. (1983) and Levkov et al. (1992), are based on the approach described in Lin et al. (1983). More precisely, collection efficiency of aggregation depends on snow crystal size according to Lohmann (2004), collection efficiency of accretion is temperature dependent following Levkov et al. (1992), while collection efficiency of self-collection is constant like in Levkov et al. (1992). It is assumed that ice crystals melt instantaneously (MELT) as soon as ~~temperatures are~~ temperature is above  $0^{\circ}\text{C}$  ~~(MELT)~~.

**Sources and sinks of ice crystals.** Sedimentation (SEDI) is a physical process which impacts ICNC by vertically redistributing the ice crystals. Although it does not really produce or remove ICs, it can be considered as source or sink relative to a selected region or period. SEDI includes also the sublimation of falling ICs which encounter an ice subsaturated region and are converted into cloud droplets.

It is important to mention that the CLOUD submodel includes also some ICNC tendencies which are defined only with the aim of assuring the physical realism of some processes or parameterizations (e.g. the ICNC value must be smaller than the maximal threshold of  $10^7$ ).

### 2.3.2 Numerical tendencies

The CLOUD submodel also includes ICNC tendencies that impose specific values when particular conditions are satisfied. For example, if ICNC exceeds an upper threshold of  $\text{ICNC}_{\text{max}} = 10^7 \text{ m}^{-3}$  ~~at each model integration time~~ ). However, since these

Tendency	Description	Temperatu
DETR-minmax0	<del>Convective detrainment</del> The minimal value allowed for ICNC is imposed ( $ICNC_{background} = 10^{-12} m^{-3}$ )	$T < -35^{\circ}C$
minmax1	<del>Ice nucleation</del> The maximal ICNC correction term is imposed ( $ICNC_{max} = 10^7 m^{-3}$ )	$-10$
minmax2	The minimal ICNC correction term is imposed ( $ICNC_{min} = 10 m^{-3}$ )	$10^{-1}$
minmax3	ICNC is equal to concentrations of the new ICs produced in the cirrus regime (1)	$T < -35^{\circ}C$
minmax4	Instantaneous freezing-ICNC <sub>min</sub> is imposed	$T < -35^{\circ}C$
minmax5	Ice nucleation in the mixed-phase regime-ICNC is equal to $ICNC_{background}$ (2)	$-35^{\circ}C < T < 0^{\circ}C$
minmax6	Secondary ice production- $ICNC_{background}$ is guaranteed	$-8^{\circ}C < T < 0^{\circ}C$
minmax7	Removal processes can decrease ICNC at maximum by the same value ICNC	0
minmax8	$ICNC_{background}$ is guaranteed	$10^{-2}$
minmax9	$ICNC_{min}$ is imposed	$10^{-1}$

**Table 2.** Numerical ICNC tendencies defined in the CLOUD submodel. The third column shows the order of magnitude (in  $m^{-3}s^{-1}$ ) of the global means computed with the REF simulation. (1) when the condition (cloud cover > 0 & cloud ice >  $10^{-12} kg kg^{-1}$  &  $ICNC < ICNC_{min}$ ) is true; (2) when the condition (cloud cover > 0 & cloud ice >  $10^{-12} kg kg^{-1}$ ) is false.

Years			
	<i>Cirrus regime</i>	<i>Mixed-phase regime</i>	
SELF-REF	Self-collection-BN09	$T < 0^{\circ}C$ cnt: LD06 ; imm&dep: P13	5 years (around 2000)
AGGR-PRES	Aggregation-KL02	$T < 0^{\circ}C$ cnt: LD06 ; imm: LD06	5 years (around 2000)
ACCR-FUT	Accretion-BN09	$T < 0^{\circ}C$ cnt: LD06 ; imm&dep: P13	5 years (around 2080)
NOicncmax	BN09	cnt: LD06 ; imm&dep: P13	1 year (around 2000)
SEDI-NOfree	Sedimentation-BN09	$T < 0^{\circ}C$ cnt: LD06 ; imm&dep: P13	1 year (around 2000)

**Table 3.** ICNC tendencies (or rates) defined in the CLOUD submodel. The first column contains the abbreviations associated with each tendency; the second column describes the (micro)physical processes associated with each tendency; the third column specifies the temperature range in which the processes occur “cnt” and “imm&dep” stand for contact nucleation and immersion & deposition nucleation, respectively.

210 “numerical tendencies”, the ICNC value is replaced by  $ICNC_{max}$ , forcing a sudden decrease of ICNC within one time step. These correction terms do not have their own physical meaning, they are not considered in this work. a physical meaning and we will refer to them as *numerical tendencies* (Table 2). Their role has rarely been addressed in the literature.

### 3 Setup of simulations

#### 215 4 Setup of simulations

The simulations in this study have been performed at T42L31ECMWF resolution, which corresponds to a spherical truncation of T42 (i.e. quadratic Gaussian grid of approximately  $2.8^\circ \times 2.8^\circ$ , in latitude and longitude) and 31 vertical hybrid pressure levels up to ~~10 hPa (about 25 km)~~ 10 hPa (about 25 km). The model time step is 20 minutes, and the model results are stored with a frequency of 5 hours. The simulations ~~are 2-years long~~ run for 6 years: the first year has been considered spin-up time, while  
220 the ~~second year has~~ next five years have been used for the analysis. Two periods are taken into account: the years ~~2000-2001~~ 2000-2005 to represent present-day conditions and the years ~~2080-2081~~ 2080-2085 to represent a ~~future period~~ global warming scenario. The simulations are forced by prescribed sea surface temperatures (SSTs) and sea-ice concentrations (SICs). SSTs and SICs are provided by the Hadley Centre Global Environment Model version 2 – Earth System (HadGEM2-ES) Model (Collins et al., 2011): the historical simulation with HadGEM2-ES is used for the present period, while the RCP6.0 simu-  
225 lation is considered for the future (~~like in the simulation RC2-oc01 of the ESCiMo project described in Jöckel et al., 2016~~) (like in the RC2-oc01 simulation of the ESCiMo project described in Jöckel et al., 2016). Aerosols are emitted offline using monthly emission files based on the AEROCOM data set, such as for mineral dust, secondary organic aerosol, and sea salt (like in Pozzer et al., 2012), or a combination of the ACCMIP (Lamarque et al., 2010) and RCP 6.0 scenario (Fujino et al., 2006), such as for black carbon and organic carbon with biomass burning and anthropogenic origins.

230 The simulations carried out in this study are one reference run and two sensitivity case studies (Table 3). The reference run (REF) simulates recent conditions and applies the ice nucleation parameterizations BN09 and P13 in the cirrus regime and mixed-phase regime, respectively (like in Bacer et al., 2018). REF will be analysed in order to quantify the rates of ice ~~(micro)physical~~ microphysical processes in cold clouds and define their relative importance. Another simulation (PRES) ~~which~~ refers to the same period but uses different ice nucleation schemes ~~has been performed to analyse the effects on the~~  
235 ~~ICNC tendencies due to a different choice of parameterizations in order to understand the effect of parameterization choice~~. In particular, the ~~simulation PRES~~ PRES simulation uses KL02 ~~and LD06~~ in the cirrus regime and LD06 in the mixed-phase regime, ~~respectively~~. Finally, the simulation representing the future period (FUT) has been run with the same model ~~set-up of~~ REF, ~~but it considers the emissions of~~ setup as REF but with the RCP6.0 emission scenario. The comparison between FUT and REF ~~allows will allow~~ us to estimate the changes ~~of the cold cloud (micro)physical processes according to in cold cloud~~  
240 microphysical processes under a global warming scenario.

~~Cirrus regime Mixed-phase regime REF BN09 P13 PRES KL02 LD06 FUT BN09 P13 Simulations carried out and analysed in this study. Additionally, two 2-year test simulations (2000 for spin-up time and 2001 for the analysis) have been run (Table 3). Both tests use the same setup as REF. In NOicnmax, the condition that ICNC must be lower than ICNC<sub>max</sub> at each model time step (i.e. the numerical tendency minmax1) is dropped, allowing us to investigate the impact of the largest numerical tendency (Table 2). In NOfree, supercooled cloud droplets can remain liquid also at temperatures lower than  $-35^\circ\text{C}$  in order to understand the influence of the FREE tendency.~~



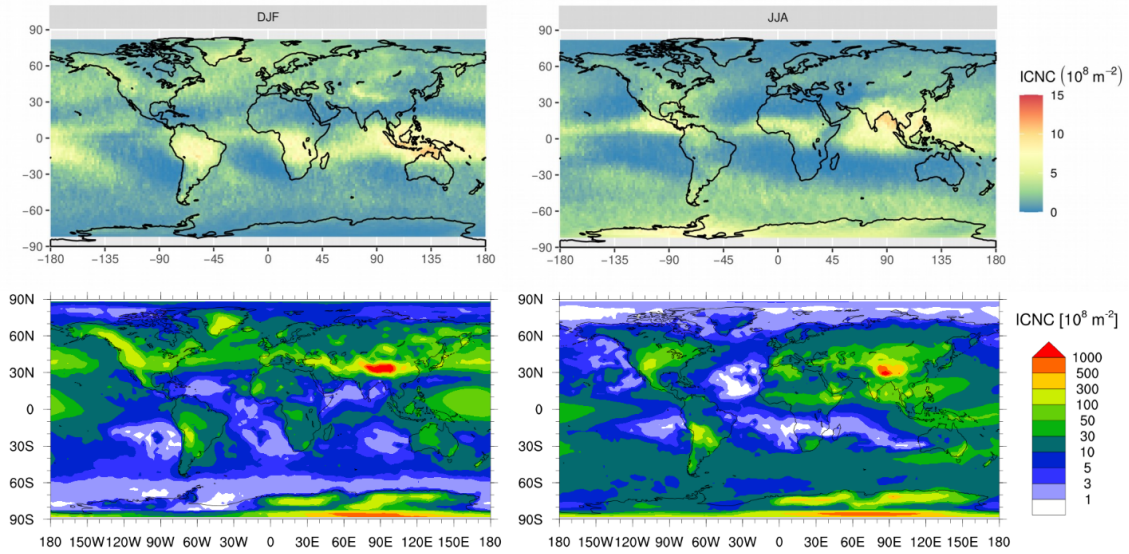


**Figure 1.** Mean spatial distribution of vertically integrated ICNC burden for the DJF and JJA seasons. (*Top*) In-cloud ICNC burden retrieved by DARDAR-Nice (2006–2017) averaged in a  $2^\circ \times 2^\circ$  grid. (*Bottom*) In-cloud ICNC burden computed by EMAC (5-hour output greater than zero were considered in the average).

#### 4 Model results and evaluation of ICNC

In this section, the ICNC obtained with the EMAC model is investigated and evaluated through comparisons to satellite ICNC retrievals by DARDAR (lidDar-raDAR)-Nice (Gryspeerd et al., 2018; Sourdeval et al., 2018). This satellite product uses the sensitivity contained in combined space-borne lidar-radar measurements in order to constrain the parameters of the particle size distribution (PSD) then used to infer the ICNC by direct integration from a particle size of  $5 \mu\text{m}$ . DARDAR-Nice retrievals are provided at vertical and horizontal resolutions of 60 m and 1.4 km, respectively. This data set has been thoroughly evaluated against a large variety of in-situ measurements (Sourdeval et al., 2018; Krämer et al., 2020), to find an overall agreement within a factor of two at cirrus temperatures. However, it should be noted that an overestimation of ICNC at warmer temperatures is possible due to the misrepresentation of the PSD bi-modality by the satellite retrieval method and of optical properties of mixed-phase clouds.

Figure 1 shows the spatial distributions of the ICNC burden during winter (DJF) and summer (JJA) seasons for both a 10-year climatology of DARDAR-Nice retrievals and model results. The satellite products present high ICNC values mainly in deep convective regions as well as in mid-latitudes during winter months, possibly due to increased ice nucleation rates associated with high wind velocities. Such features are in most parts also observed in the patterns of the model ICNC burden distribution, which is in good overall agreement with the satellite retrievals. However, absolute values differ by about an order of magnitude, with ICNC burdens up to about  $10^9 \text{ m}^{-2}$  in DARDAR-Nice and  $10^{10} \text{ m}^{-2}$  in EMAC in most of these two regions. A larger discrepancy can be seen over Antarctica, where the model overestimates ICNC probably due to very



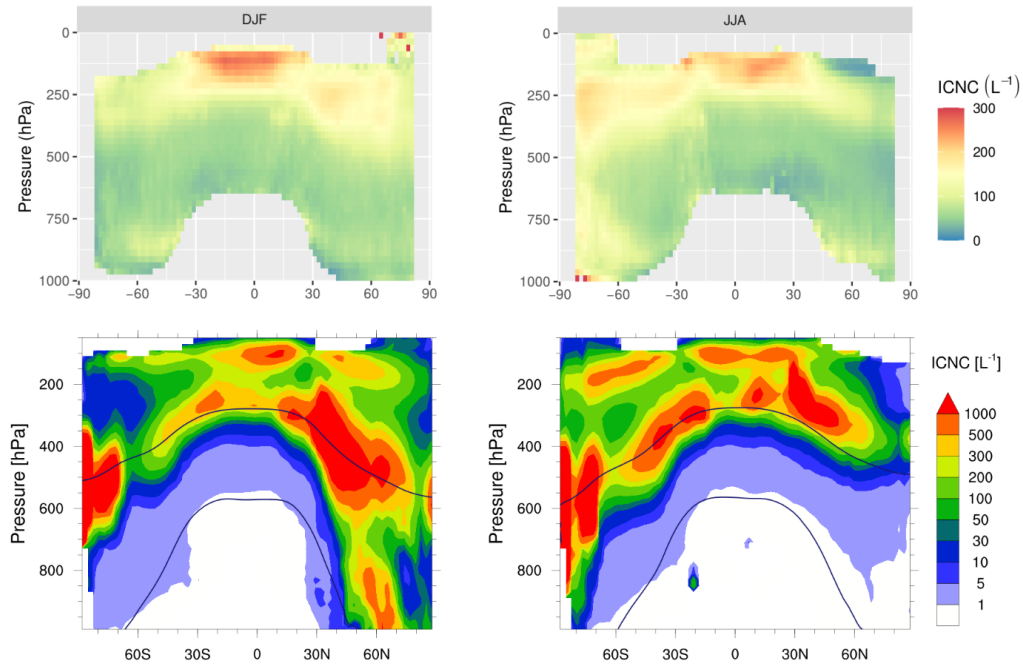


**Figure 2.** Zonal means of in-cloud ICNC for the DJF and JJA seasons by DARDAR-Nice (*top*) and EMAC (*bottom*); the isotherms at 0°C and −35°C are seasonal means.

low temperatures (lower than −35°C most of the year) and high supersaturation levels. Even higher values, up to  $10^{11} \text{ m}^{-2}$ , are simulated by EMAC in mountainous regions. ICNCs of the same order of magnitude can be found in other modeling studies (e.g. Kuebbeler et al., 2014; Gasparini and Lohmann, 2016; Bacer et al., 2018). Although increases of ICNC around steep orography are noticed in the satellite products, and are consistent with strong homogeneous freezing in the strong uplifts associated with mid-latitude jets during winters, they mainly occur right between the homogeneous nucleation threshold and −60°C (Sourdeval et al., 2018), where ICNC locally reaches up to  $300 \text{ L}^{-1}$  (nearly three times the surrounding values). Therefore, these features do not strongly appear in the ICNC burden nor in the corresponding zonal ICNC profiles shown in Figure 2 (top). These profiles exhibit ICNC values that are consistent with the aforementioned observations, i.e. high ICNC values (up to  $300 \text{ L}^{-1}$ ) in the tropics and in the mid-latitudes (up to  $150 \text{ L}^{-1}$ ). Sharp increases of ICNC values (from about 50 to above  $100 \text{ L}^{-1}$ ) are also noted in the vertical profiles between 500 and 300 hPa, according to the activation of homogeneous nucleation. These features are consistent with what is modeled in EMAC (Figure 2, bottom), both in terms of patterns and absolute values. Nevertheless, higher ICNC values, up to  $1000 \text{ L}^{-1}$ , tend to occur at lower altitude in the troposphere, seemingly related to orographic features. While uncertainties remain on the absolute ICNC by DARDAR-Nice, it should be noted that such high values are only rarely reported from in-situ measurements (Krämer et al., 2016, 2020), therefore it is likely that EMAC overestimates ICNC.

## 5 Results and Discussion

### 5 ICNC tendency results

#### 5.1 Global distributions

##### 5.1 Global statistics

The global distributions of the vertically integrated tendencies for the REF simulation are shown in Figure 5, and the global means and the standard deviations of the tendencies are shown in Table 4. In cirrus clouds, the largest source of ICs is the instantaneous freezing of supercooled cloud droplets, followed by convective detrainment and then ice nucleation (including homogeneous and heterogeneous nucleation). Both DETR and NCIR are higher over regions that experience strong convective activity, e. g. the Intertropical Convergence Zone (ITCZ) and In this section, we analyse the role of each tendency in terms of extent (Table 4) and relative contribution (Figure 3) at the global scale. In all simulations, the Tropical Warm Pool (TWP). DETR is higher over land than over ocean because the land-ocean differences in the thermodynamic profiles below the freezing level produce stronger updrafts over land (Del Genio et al., 2007). Moreover, DETR tends to be smaller off the west coasts of South America, Africa, and Australia where SSTs are colder and stratocumulus decks dominate. FREE shows particularly high values over continents and especially over mountainous regions, where liquid cloud droplets are efficiently transported by strong updrafts up to levels where the temperature is lower than  $-35^{\circ}\text{C}$  and freeze. Thus, FREE contributions are high but localised and their annual mean is larger than DETR and NCIR while the FREE annual median is negligible. This is shown in Table 4 (and Subsection 5.4), where the FREE distribution presents the highest variability although its 99th percentile is still negligible. largest source of ICs is the instantaneous freezing, whose mean tendency is of the order of  $10^2 \text{ m}^{-3}\text{s}^{-1}$  with a relative contribution of about 50%. FREE is followed by convective detrainment and homogeneous and heterogeneous ice nucleation in the cirrus regime. In mixed-phase clouds, the largest IC source is heterogeneous nucleation, followed by secondary ice production, with a distribution (not shown) that is similar to the one of NMIX and whose global mean is lowest among the IC sources (Table 4). NMIX is influenced by the orography (the largest tendencies occur over the Rocky Mountains, the Andes, and the Himalayas) and the abundance of the INPs responsible for heterogeneous nucleation via P13 (i. e. mineral dust, black carbon, soluble organics, and bioaerosols); in fact, high NMIX values are found over the main deserts and downwind areas (e. g. the Saharan region and the Arabian peninsula) and, more generally, in Asia due to high emissions of black carbon and of dust from the Gobi Desert. Globally, FREE; they are of the order of  $10^{-2} \text{ m}^{-3}\text{s}^{-1}$ , and their relative contribution is less than 0.1%. Globally, the hierarchy of IC sources in the REF simulation is  $\text{FREE} > \text{DETR} > \text{NCIR} > \text{NMIX} > \text{SECP}$  is the hierarchy of IC sources in REF (Table SECP (Table 4). Our results are in agreement with the recent study of Muench and Lohmann (2020), who also found that homogeneous freezing and convective detrainment are the dominant sources of ICs. Aggregation is the major physical removal process of ICs in all simulations, of the order of  $10 \text{ m}^{-3}\text{s}^{-1}$ , with about double the rate of accretion. Self-collection and melting are much less efficient sinks, on average two to four orders of

310 magnitude lower than AGGR, respectively, with a relative contribution smaller than 0.1%. Hence, the hierarchy of IC sinks in REF is AGGR > ACCR > SELF > MELT (Table 4).

Among the IC removal processes (Figure 5), aggregation is the largest IC sink, followed by accretion and sedimentation; self-collection and melting tendencies. At this point, the important role of the numerical tendencies must be stressed. While most numerical tendencies have contributions to ICNC smaller than any of the microphysical tendencies (Tables 2 and 4), a few have non-negligible contributions (e.g. minmax1,3,4,5). As a result, the sum of all negative numerical tendencies (MINMAX-) is higher than AGGR, for example, contributing more than 30% to IC removal, relative to only 10% from AGGR. These correction terms are not often analysed, but we highlight their importance here. Ice microphysics parameterizations may get the right answer for the wrong reason because of these numerical artifacts.

We can illustrate the impact of these numerical tendencies by examining the test simulation NOicncmax. The imposition of ICNC<sub>max</sub> (not shown) are on average two and four orders of magnitude lower, respectively (Table minmax1) is the dominant negative numerical tendency (Table 2). Without this condition, MINMAX- decreases by an order of magnitude, and ACCR and AGGR become the dominant sink terms (Figure 3). Moreover, while there is a quite balanced division between IC sources and sinks for the other simulations, the source terms dominate in NOicncmax at 60%. We have not considered the transport and sedimentation tendencies here and so cannot determine whether the clouds can realistically dissipate in the absence of the minmax1 tendency. However, we can emphasise the impact of this numerical tendency as the global mean ICNC in the NOicncmax simulation is three times larger than that in the REF simulation (Table 4). All sinks show similar patterns, as active aggregation and accretion produce ICs large enough to sediment out, faster than depositional growth. The sink tendencies are higher over land and influenced by the orography. They are also high throughout the mid-latitudes (between 30° and 60°) and over Antarctica, following the vertically integrated ICNC pattern (Figure 4). Therefore, an enforced ICNC upper bound of  $10^7 \text{ m}^{-3}$  significantly dampens the ICNC produced globally (Figure S1 in the Supplement) in the Supplement).

We also investigated the case in which the dominant source, FREE, does not take place. The results of the test simulation NOfree show that the ICNC tendencies remain of the same magnitude (Table 4). The suppression of instantaneous freezing does allow detrainment to become the leading source of ICs (Figure 3). ICNC also strongly decreases in the middle and lower troposphere (Figure S1), while global mean ICNC drops by an order of magnitude with respect to the REF simulation (Table 4). In contrast, CDNC increases by 10% on average (not shown), as cloud droplets that would otherwise transform into ICs in REF remain in the liquid phase in NOfree.

Finally, for each microphysical process, we computed the occurrence of the tendency values greater than zero (Figure 4). We find that all distributions are highly asymmetric and, in particular, left-skewed. Only MELT shows a bell-shaped distribution; but even in this case, the median is lower than the mean suggesting a tail to the left of the distribution. A few processes are characterised by multimodal distributions; for example, the distribution of DETR is bimodal, while the distributions of SELF, AGGR, and ACCR are trimodal.

## 5.2 Spatial distributions

Tendency	REF		PRES		FUT		
	Mean	StDev	99th/1st-Mean	StDev	99th/1st-Mean	StDev	
DETR	<del>1.87</del> 1.8e+00	<del>53.90</del> 6.2e+01	<del>11.14</del> 1.5e+00	<del>1.63</del> 5.6e+01	<del>50.61</del> 1.7e+00	<del>1.51</del> 5.6e+01	<del>1.</del>
NCIR	<del>0.52</del> 6.0e-01	<del>8.77</del> 9.9e+00	<del>10.79</del> 4.7e+01	<del>38.71</del> 2.1e+03	<del>1734.19</del> 5.0e-01	<del>43.48</del> 7.2e+00	<del>0</del>
FREE	<del>77.69</del> 1.1e+02	<del>2837.23</del> 3.6e+03	<del>0.00</del> 9.2e+01	<del>50.55</del> 3.3e+03	<del>2267.82</del> 7.8e+01	<del>0.00</del> 3.0e+03	<del>57.</del>
NMIX	<del>0.11</del> 5.6e-02	<del>3.74</del> 2.6e+00	<del>0.80</del> 2.4e-01	<del>0.74</del> 2.1e+01	<del>42.35</del> 3.9e-02	<del>1.42</del> 2.0e+00	<del>0</del>
SECP	<del>0.04</del> 1.7e-02	<del>0.67</del> 3.4e-01	<del>0.34</del> 1.6e-02	<del>0.05</del> 3.3e-01	<del>0.68</del> 1.5e-02	<del>0.38</del> 3.1e-01	<del>0</del>
MELT	<del>-1.5e-03</del>	<del>9.6e-01</del>	<del>-1.4e-03</del>	<del>9.9e-01</del>	<del>-1.4e-03</del>	<del>1.1e+00</del>	<del>3.</del>
AGGR	<del>159.89</del> 1.7e+01	<del>37.37</del> 4.9e+02	<del>2.74</del> 1.6e+01	<del>166.00</del> 4.3e+02	<del>22.85</del> 1.3e+01	<del>4.3e+02</del>	
MELT-ACCR	<del>0.00</del> 9.1e+00	<del>0.95</del> 3.3e+02	<del>0.00</del> 8.2e+00	<del>0.00</del> 2.9e+02	<del>0.73</del> 6.8e+00	<del>0.00</del> 2.6e+02	<del>0.0</del>
AGGR-SELF	<del>-17.59</del> 1.1e-01	<del>603.30</del> 3.6e+00	<del>-89.16</del> 1.0e-01	<del>-14.67</del> 3.1e+00	<del>515.83</del> 8.3e-02	<del>-131.77</del> 3.1e+00	<del>-13.</del>
MINMAX+	<del>-9.07</del> 4.9e-02	<del>372.28</del>	<del>-38.18</del> 3.9e-03	<del>-7.26</del>	<del>318.18</del> 4.6e-02	<del>-43.64</del>	<del>-7</del>
SELF-MINMAX-	<del>-0.10</del> 6.7e+01	<del>3.94</del>	<del>-0.36</del> 9.7e+01	<del>-0.08</del>	<del>3.29</del> 4.6e+01	<del>-0.63</del>	<del>-0.0</del>
ICNC	<del>-14.75</del> 2.5e+02	<del>421.67</del> 7.3e+03	<del>-89.23</del> 2.6e+02	<del>-12.38</del> 6.5e+03	<del>320.19</del> 1.8e+02	<del>-162.03</del> 5.9e+03	<del>-10.</del>
Hierarchy (REF and FUT)							Sour

**Table 4.** Statistics computed on the by using 5-hourly ICNC tendencies; output of the 5-year simulations REF, PRES, and FUT : global and the 1-year simulations NOicncmax and NOfree. Global means and standard deviations, 99th/1st percentiles for sources/sinks of ICs (are in  $\text{m}^{-3}\text{s}^{-1}$ ). Only the 99th percentiles are shown for the sources as the 1st percentiles are zero; vice versa, only the 1st percentiles are shown for the sinks as the 99th percentiles are zero. Median values are zero tendencies and in  $\text{L}^{-1}$  for all grid-averaged ICNC tendencies. (Note that SEDI MINMAX+ and SEDI take into account only MINMAX- are the sum of the means of positive and negative values numerical tendencies, respectively (according to Table 2). The last two rows summarise the hierarchy of the ICNC tendencies in REF and FUT.

The global distributions of the vertically integrated tendencies for the REF simulation are shown in Figure 5. Both DETR and NCIR are higher over regions that experience strong convective activity, e.g. the Intertropical Convergence Zone (ITCZ) and the Tropical Warm Pool (TWP). DETR is higher over land than over ocean because the land-ocean differences in the thermodynamic profiles below the freezing level produce stronger updrafts over land (Del Genio et al., 2007). DETR and NCIR tend to be smaller off the west coasts of South America, Africa, and Australia where SSTs are colder and stratocumulus decks dominate. FREE mostly occurs in extratropical regions, where warm conveyor belts can form, and over continents. In particular, FREE shows high values over mountainous regions, where liquid cloud droplets are efficiently transported by strong updrafts up to levels where the temperature is lower than  $-35^{\circ}\text{C}$  and freeze, and over Antarctica, where the temperature is lower than the freezing threshold for most of the year. The high values of FREE could be responsible for the ICNC overestimation mentioned in Section 4. Since FREE contributions are high but localised, their annual mean is larger than DETR and NCIR while the FREE annual median is negligible (Subsection 5.4). NMIX is influenced by the orography and the abundance of the INPs responsible for heterogeneous nucleation in the P13 scheme: the largest tendencies occur over the Rocky Mountains, the Andes, the Himalayas, and over and downwind of large deserts (e.g. the Saharan region and the Arabian peninsula). NMIX is also large over Asia due to high emissions of black carbon and dust from the Gobi Desert. All IC sinks show similar patterns

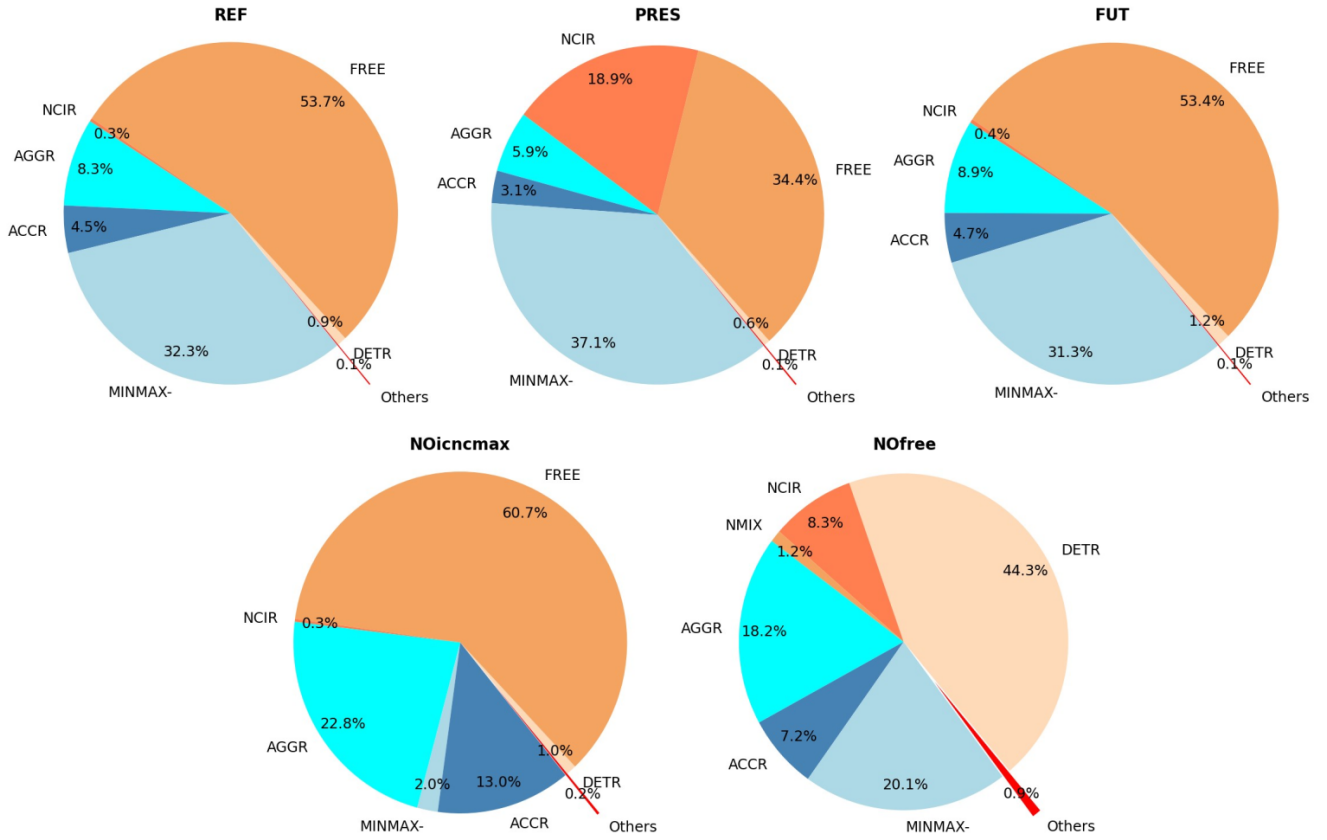


**Figure 3.** Annual-mean relative contributions of the vertically-integrated-mean tendencies in Table 4. The sector “Others” of the pie charts includes NMIX, SECP, MELT, SELF, MINMAX+ (apart in  $10^5 \text{ m}^{-2} \text{ s}^{-1}$  NOfree, where NMIX is represented independently) for the. Warm tones of colors indicate sources and sinks of ICs, while cold clouds (REF-simulation) tones of colors indicate sinks of ICs.

globally: they are higher over land and influenced by orography. They are also high throughout the mid-latitudes and over Antarctica, following the vertically integrated ICNC pattern (Figure 1).

### 5.3 Annual-zonal Zonal means

360 We next explore the zonally averaged profiles of IC sources and sinks in the REF simulation (Figures 6 and 7). We clearly see that ice nucleation in the cirrus regime (NCIR) is the dominant source of ICs in the upper troposphere (at pressures lower than about 350 hPa) and has 350 hPa. NCIR presents a maximum in the tropics, coincident with that in the maximum of ICNC (Figure S2-S1 in the Supplement). In fact, upper-level gravity wave activity, particularly strong in the tropics, can generate temperature fluctuations responsible for strong nucleation tendencies, where temperature is very low ( $T < -80^\circ\text{C}$  on average) and ice supersaturation is high ( $s_i > 36\%$  on average, not shown). NCIR is slightly higher in the Southern Hemisphere (SH) than in the Northern Hemisphere (NH), where heterogeneous nucleation occurs more frequently

365

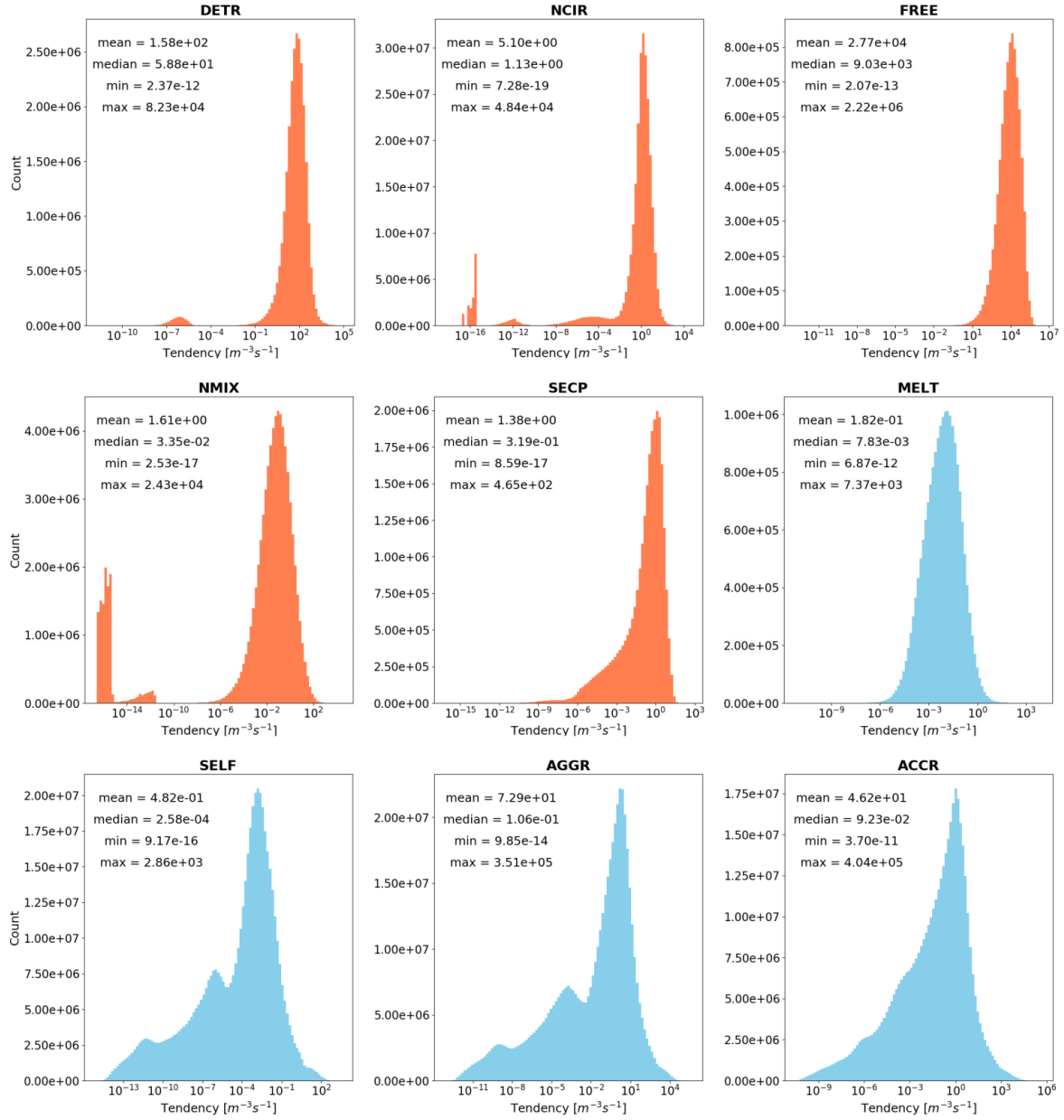


**Figure 4.** Occurrence and statistics of ICNC tendencies (REF). The bar charts are computed with 5-hour output data distributed in 100 logarithmic bins. For each tendency, only values greater than zero have been considered in the analysis (absolute values are used for the sinks). The vertical axis shows the occurrence in linear scale, the horizontal axis shows the tendency values in logarithmic scale. Warm tones of colors indicate sources of ICs, while cold tones of colors indicate sinks of ICs.



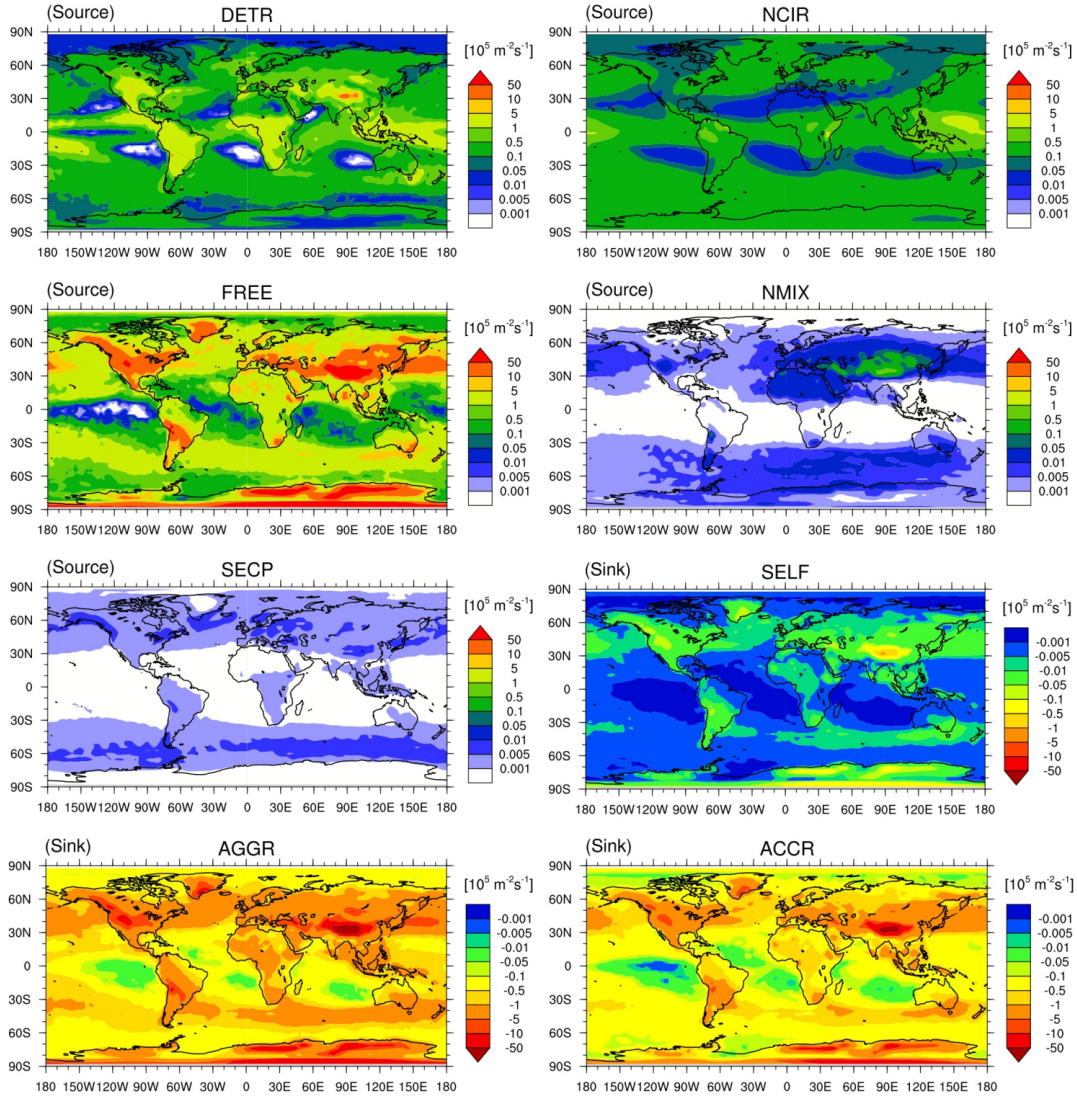


**Figure 5.** Annual means of the vertically integrated tendencies (in  $10^5 \text{ m}^{-2} \text{ s}^{-1}$ ) for sources and sinks of ICs in cold clouds (REF).

and could suppress homogeneous nucleation. DETR contributes to produce ICs at temperatures  $T < -35^\circ\text{C}$  (i.e. in the cirrus regime) especially in-between the mid-latitudes ( $50^\circ\text{N}$  and  $50^\circ\text{S}$ ), as illustrated in Figure 5. By definition, detrained cloud condensate is in the ice phase when  $T < -35^\circ\text{C}$  (see Subsection 2.3.1), however, Coopman et al. (2020) have recently found that glaciation of isolated convective clouds over Europe usually occurs at higher temperature ( $-22^\circ\text{C}$ ). Hence, the temperature threshold for the cloud thermodynamic phase transition in the CLOUD submodel could be too low and contribute to an underestimation of ICNC in the mixed-phase regime with respect to observations (as discussed in Section 4). FREE is the highest largest source of ICs close to the area of transition between cirrus regime and transition from the cirrus

to mixed-phase regime and especially outside the tropics. In mixed-phase clouds, NMIX dominates in the mid-latitudes, with values higher in the Northern Hemisphere (NH) than in the Southern Hemisphere (SH) because of higher concentrations of INPs (e.g. Hoose et al., 2010; Liu et al., 2012) and cloud droplets (e.g. Karydis et al., 2017). INP and cloud droplet concentrations (e.g. Hoose et al., 2010; Liu et al., 2012; Karydis et al., 2017). While NMIX affects the whole mixed-phase regime (i.e. the area between the two isotherms in Figure 6), SECP is more concentrated active at lower altitudes, as the Hallett-Mossop process occurs at  $-8^{\circ}\text{C} < T < -3^{\circ}\text{C}$ . Sedimentation, which is actually a vertical redistribution of ICs, behaves as a source of ICs (i.e. SEDI+) mostly in the mixed-phase regime, where both the number and size of ICs are non-negligible. On the contrary, SEDI+ is low at upper levels because the crystals are too small to fall out and at lower levels because the number of ICs is a small. The global mean of SEDI+ is of the same order of magnitude of DETR, so that the hierarchy of all IC sources is: FREE > SEDI+ > DETR > NCIR > NMIX > SECP (Table 4). In general, the zonal means of IC sources, but also their global distributions, are in agreement with the results of Muench and Lohmann (2020).

On average, the IC sinks AGGR, ACCR, and SEDI- show similar vertical distributions (Figure 7). AGGR and ACCR are qualitatively similar (Figure 7). Nevertheless, sedimentation is the most significant IC sink in the upper troposphere and in the lower troposphere, extending to higher and lower altitudes than either AGGR or ACCR. Interestingly, the sedimentation sink (SEDI-) is almost four times larger than the sedimentation source (SEDI+) (Table 4). While SEDI- involves very many small ICs falling from high latitudes, SEDI+ occurs at lower altitudes where ICs have already undergone growth processes like aggregation that reduce their number. All sink processes but except melting show higher values along the transition zone between the two cloud regimes, in particular in the NH and over the Antarctica where ICNCs are higher (Figure S2 in the Supplement). SEDI- and AGGR extend 1). AGGR extends to lower altitudes in the NH than in the SH. Overall, the hierarchy of IC sinks is: AGGR > SEDI- > ACCR > SELF > MELT, where ACCR and SEDI- are of the same order of magnitude (Table 4).

It must be noted that stressed that the IC sources and sinks of Figures 6 and 7 cannot be expected to balance because the tendency due to advective, turbulent, and convective transport (i.e. for two reasons. First, the tendencies of physical processes are not computed in this study, i.e. transport due to advection, turbulence, and convection and sedimentation ( $R_{transp}$  and  $R_{sed}$  in equation (1)), respectively). In particular,  $R_{transp}$  is not computed in the CLOUD submodel but derives from various submodels in EMAC, e.g. CVTRANS (Tost et al., 2010) and E5VDIFF (Roeckner et al., 2004), and is not shown here. Second, numerical tendencies also affect ICNC at each model time step and play a significant role in the ICNC budget (as discussed in Subsection 5.1).

#### 5.4 Regional results

The ICNC tendencies are further analysed at the regional scale. The annual medians of the tendencies are computed in bins of 20 hPa for the following areas (whose coordinates are shown in Figure S1 in the Supplement): considering areas over the Sahara, Amazon, Europe, Central Europe, North Atlantic Ocean, and Indian Ocean, and the resulting vertical profiles are shown in Figure 8. In order to appreciate the differences among the microphysical process profiles, only the areas Southern Indian Ocean (Figure S2 in the Supplement). For each region, the medians of the tendencies are computed in bins of 25 hPa



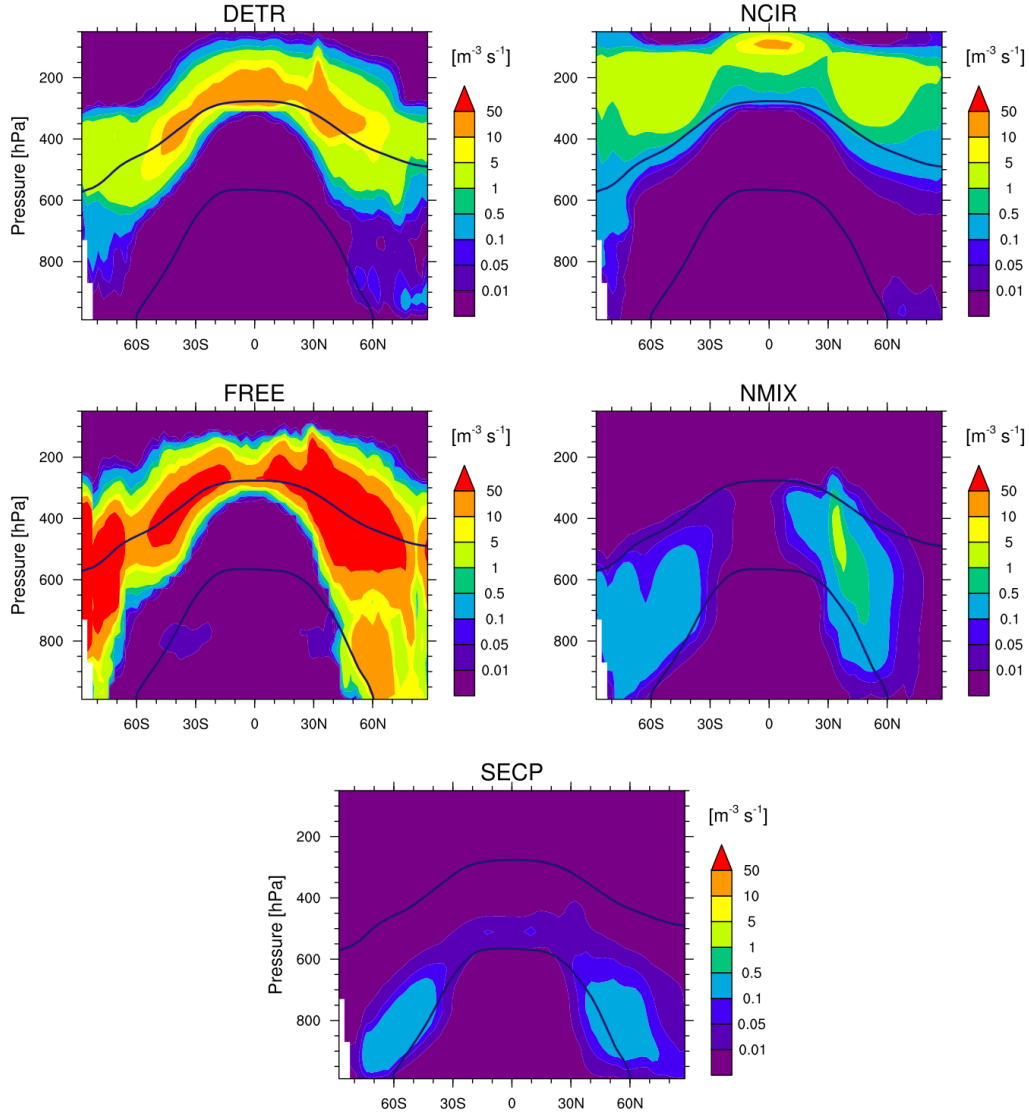


**Figure 6.** Annual zonal means of the tendencies associated to the IC sources in cold clouds (REF~~simulation~~). The isotherms at 0°C and −35°C are annual means. ~~(Note that SEDI here takes into account only positive values.)~~

~~and only in grid-boxes~~ where  $\text{ICNC} > 1 \text{ L}^{-1}$  ~~are considered for the computations of the medians, therefore, the tendencies must be compared relative to the ICNC profiles (also shown in Figure 8) as they do not represent absolute values. It appears that~~  
410 ~~ICNC is higher over land than over ocean and the~~ (Figure 8). The tendencies of different regions must then be compared along  
with the associated ICNC profiles, as a different number of grid-boxes is used for the statistics at the same vertical level. The  
lower the latitude, the higher the altitude associated with the peak in the ~~tendency profiles~~ ICNC profiles, as expected. Relatively  
colder surface temperatures over Europe mean both that the European ICNC ~~peak~~ ~~maximum~~ occurs at a lower pressure level

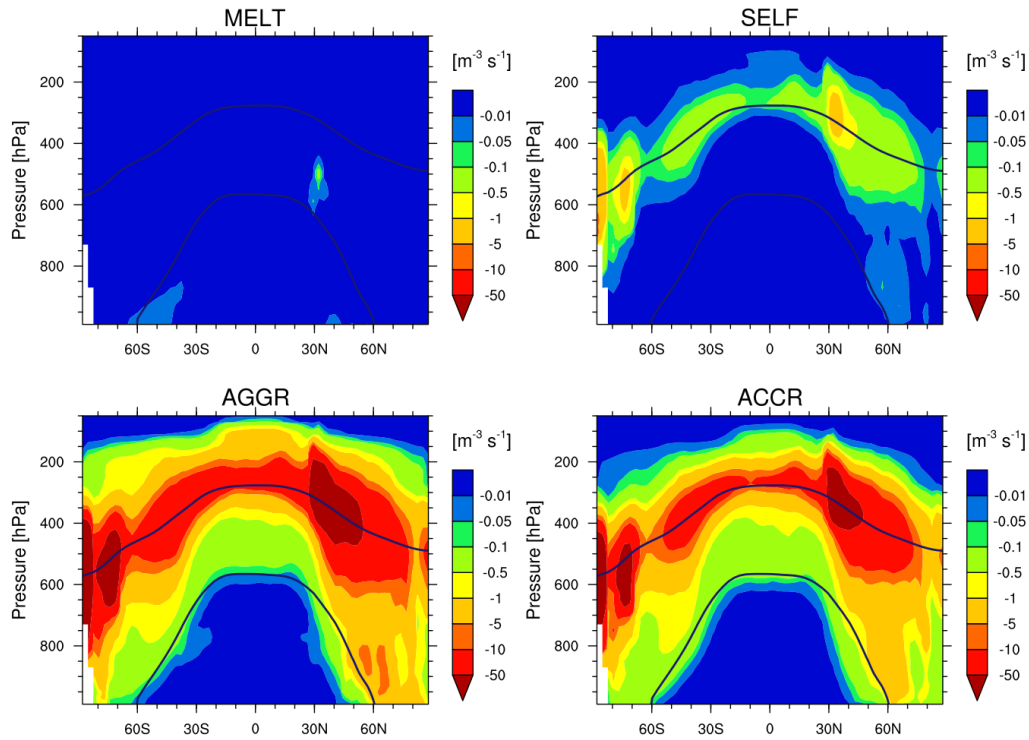


**Figure 7.** Annual zonal means of the tendencies associated to the IC sinks in cold clouds (REFsimulation). The isotherms at 0°C and −35°C are annual means. (Note that SEDI here takes into account only negative values.)

and that non-zero tendencies extend down to the surface. It is interesting that sedimentation shifts from being a sink in the upper troposphere to a source when NCIR tends to zero, in all regions

In all regions, the sinks look similar: AGGR is a stronger removal process than ACCR, and its maximum is at higher altitudes than ACCR. The sources are more regionally variable. In the middle and lower troposphere, ICs derive especially from sedimentation and over Europe, the Amazon and the maritime regions, ICs are generated by secondary ice production; however, the contribution to ICNC of ice nucleation in the mixed-phase can be more important in some regions. In fact, NMIX plays a major role at pressures higher than 600 hPa. The great relevance of secondary ice in regions with modest updrafts and aerosol loadings has been reported in several studies (e.g. Sullivan et al., 2016; Field et al., 2017). In contrast, over the Sahara region because of the new ICs formed heterogeneously from mineral dust, NMIX is the dominant IC source, given the large mineral dust loading. The regional means (Table of the ICNC tendencies and their relative contributions (Table S1 and Figure S3 in the Supplement) computed for this region indicate show that NMIX is more important than NCIR and SECP, changing even slightly higher than NCIR over Sahara and also over Europe, i.e. over highly polluted land. Thus, in these two regions the hierarchy found at the global scale. DETR plays a role especially over low latitudes, i.e. over the Sahara and Amazon regions, where strong convective activity is frequent (although over the Amazon only the 75th percentile is visible

while the median is close to zero). On average, DETR is more important than SEDI+ changes to  $\text{FREE} > \text{DETR} > \text{NMIX} > \text{NCIR} > \text{SECP}$ .

Over the Amazon, significant convective activity boosts the importance of DETR relative to other regions. In both their vertical profiles and relative contributions, the two oceanic areas look similar despite being subject to different aerosol conditions. ICNC in these regions (Table S1), thus altering the global hierarchy. AGGR is generally a stronger removal process than ACCR, as mentioned in the previous section, and its maximum is at higher altitudes than ACCR.

The is also less frequently larger than  $\text{ICNC}_{\text{max}}$ , as the relative contribution of MINMAX- in IND\_oce and in ATL\_oce remains low (Figure S3). Finally, we note that the medians in Figure 8 and the statistics in Table 4 and Table S1 in the Supplement indicate that ICNC tendencies are often characterised by a strong skewed distribution towards high (absolute) values so that their medians and means are very different again indicate that the microphysical tendencies are characterised by skewed distributions. This is valid especially for FREE, with its transitions from being the main source of new ICs in the mean to being a negligible source in the median.

Microphysical process tendencies and ICNC as a function of pressure computed for different regions: Amazon, Sahara, Europe, Indian Ocean, and Atlantic Ocean. The vertical profiles are annual medians computed only where  $\text{ICNC} > 1 \text{ L}^{-1}$  in bins of 20 hPa. The coloured shadows mark the areas between the 25th and the 75th percentiles whose median is close to zero (and not visible) in Figure 8.

## 5.5 Sensitivity studies

### 5.5.1 Effects due to Impact of ice nucleation scheme change

Having defined the hierarchy of the ICNC tendencies in REF, we continue with analysing the microphysical processes associated with different microphysical parameterizations. For this purpose, now to analyse how microphysical parameterizations may change this hierarchy. We replace the ice nucleation parameterizations BN09 and P13 (in the simulation REF) have been replaced by with the KL02 and LD06 in the simulation PRES. The schemes in the PRES simulation. A comparison of the ICNC tendencies between REF and PRES is displayed in Figures S3 and given in Figure S4 in the Supplement. As an expected consequence of the PRES set-up. As expected, the ice nucleation tendencies (i.e. NCIR and NMIX) exhibit the strongest differences; both increase in PRES, particularly NCIR, whose global mean rises increases by almost two orders of magnitude. This dramatic increase (Table 4). This jump in NCIR is due to the fact that LD06-KL02 parameterizes only homogeneous nucleation and disregards the competition for water vapour between homogeneous and heterogeneous nucleation and the effects of pre-existing ice crystals, producing more, smaller ICs than BN09. (A detailed comparison between the different ice nucleation parameterizations is given in Bacer et al. (2018)). At the same time, the other processes which produce new ICs are not associated with significant changes. In fact, DETR, FREE, and SECP results. The relative contribution of FREE also decreases, as the NCIR contribution increases (Figure 3), however, FREE remains the main IC source in terms of absolute values. The other source terms (DETR and SECP) do not change significantly: they decrease by less than 1% ; so that (Figure S4), and their global means are of the same magnitude as close to those computed in REF (Table 4). As a

~~result~~Overall, the application of different parameterizations for ice nucleation has only slightly changed the hierarchy of the IC sources (~~which now is~~ FREE > NCIR > SEDI+ > DETR > NMIX > SECP ). ~~Among in PRES).~~

Turning to the sinks, SEDI-, SELF, ACCR, and AGGR increase more than 5% in the upper troposphere (Figure S4). Nevertheless, ~~their overall increase is~~, but their increase is still much smaller than that of the NCIR and NMIX. ~~This can be due to the minor efficiency of these sinks when smaller ICs are involved. (It must be remembered that the change in the transport tendency has not been analysed, thus, sources and sinks cannot be expected to balance.)~~ sources. If many small ice crystals are produced, these sinks become much less efficient. The global means of the physical removal processes are almost unchanged in PRES with respect to REF (Table 4); however, we observe that the negative numerical tendencies strengthen and that the relative contribution of MINMAX- increases at the expense of ACCR and AGGR (Figure 3).

In conclusion, changing a given process parameterization can strongly influence that process tendency but may propagate weakly to other process tendencies. In particular, changing a source parameterization is expected to have only a small influence on the sink hierarchy. It is also important to note that, since parameterizations depend on model-computed quantities like vertical velocity and aerosol number concentrations as well as parameters like freezing threshold, tendencies are also strongly dependent on model setup.

### 5.5.2 Effects due to global warming

In order to estimate the global warming effect on cold cloud microphysical processes, ~~the simulations we next compare the~~ REF and FUT ~~have been compared simulations~~. The relative percentage changes of the annual zonal means of the FUT tendencies with respect to the REF tendencies are displayed in Figure 9 ~~for the IC sources and Figure S5 in the Supplement for the IC sinks. We found an upward altitude shift of the microphysical processes responsible for both the production and the~~ 9. Both microphysical tendencies for production and removal of ICs ~~under a global warming scenario. The reason is that, as~~ shift upward under global warming. As the surface temperature warms, the troposphere deepens and the lapse rate becomes less steep; ~~given~~. Given the cold temperature criteria for most ICNC processes, their contributions must shift upward in altitude to reach the same temperature regime.

All ICNC tendencies increase in intensity. The DETR, SECP, AGGR, ACCR, and SELF tendencies all increase in magnitude (up to 10%) in the upper troposphere, while they slightly decrease (about 1%) at lower altitudes ~~towards the end of the 21st century with warming~~. This is consistent with the upward shift of the freezing level indicated by the isotherms computed for FUT and in agreement with Del Genio et al. (2007). While SELF, AGGR, and ACCR increase in the “new” cirrus regime, i.e. the area delimited by the isotherm at  $-35^{\circ}\text{C}$  computed for FUT, NCIR and DETR mostly increase in the upper troposphere. In particular, DETR increases at the highest levels in the tropics as ~~convection is expected to extend deeper and carry overshooting~~ convection may occur more often or extend deeper, carrying more ICs to these altitudes. However, ~~DETR decreases by a few percent around the  $-35^{\circ}\text{C}$  isotherm where the absolute DETR contribution is largest (Figure 6). The decrease of DETR is expected~~ In contrast, right around the freezing level, DETR decreases. Upper-tropospheric static stability is expected to increase in a warmer climate ~~as an increased upper-tropospheric static stability can reduce the upper-level mass convergence in~~, reducing the mass convergence into clear-sky areas, which reduces the convective anvil cloud coverage and in turn regions

495 ~~and hence~~ the ice detrainment (Bony et al., 2016). ~~Indeed, we see a decrease in the mean upper-level divergence from the REF to the FUT simulation (Figure 10c), as well as a decrease in mean cloud fraction between 250 and 400 hPa across latitudinal bands (Figure 10b). While the detrainment increase above 200 hPa is driven by a few instances of extreme deep convection, the detrainment decrease around the melting layer is driven by mean convective behavior.~~

~~Overall, the ICNC increase in the upper troposphere with respect to recent conditions, as shown in Figure S2 in the Supplement. As a consequence, since the longwave atmospheric heating associated with cirrus clouds is a function of their emissivity and cloud base temperature (Lohmann and Gasparini, 2017), thicker cirrus clouds at higher altitudes enhance atmospheric warming and give rise to a positive feedback in response to surface warming. Moreover, as ICNC increases for a relatively fixed water vapor content in the uppermost atmosphere, NCIR decreases in the upper troposphere. This can also be understood in terms of an increasing upper-tropospheric static stability, which dampens the vertical velocity and its subgrid component input to the ice nucleation scheme, both in the mean and at the 99th percentile (Figure 10d-e). With weaker vertical motion, less supersaturation is generated to drive ice nucleation. In spite of this decreased nucleation, we see an increase in overall ICNC between 200 and 300 hPa in the FUT simulation with respect to REF, both in absolute and relative differences (Figures S1 and 10a). This increase in upper-level ICNC manifests itself as an increase between 0.1 and 0.3 K day<sup>-1</sup> of the cloud longwave radiative heating in the FUT simulation (Figure 10f). This increased upper-level heating is important as it stabilizes the atmospheric column and suppresses deep convective activity.~~

500  
505  
510

~~Although we have not shown ice crystal radii here, if ICNC were to increase at a fixed cloud ice water content, the ICs would become smaller and their fall speed decrease. A decrease in fall speeds speeds would decrease. Decreased fall speed would, in turn, translates translate to more persistent ice clouds that can warm the upper atmosphere over longer times. Indeed, along with the entrainment rate, the IC fall speed has been shown to be a crucial parameter affecting the equilibrium climate sensitivity (i.e. the surface temperature change in response to an increase of carbon dioxide concentration) (Sanderson et al., 2008).~~

515

~~At the global scale, the hierarchy of the ICNC tendencies in FUT remains the same as in As we see significant decreases in cloud fraction in the FUT simulation (Figure 10b), our results do not support such a mechanism which would counteract those associated with increased static stability. Also, while ICNC increases in a narrow vertical range between the melting layer and tropopause, the global mean ICNC decreases by almost 30% in FUT relative to REF (Table 4). Moreover, the absolute values of the annual global means computed for FUT are lower than the ones computed for REF, therefore, in the future 4); intuitively, a warmer future means less new ICs will be produced and more ICs will be removed. In fact, the global average of ICNC decreases in FUT by about 5% with respect to present days, being produced and removed. At the global scale, the hierarchy of ICNC tendencies remains the same between the REF and FUT simulations.~~

520

## 6 Conclusions

525 We studied the relative importance of cold cloud microphysical process rates (tendencies) ~~which and the unphysical corrections (numerical tendencies) that~~ affect ICNC using global simulations performed with the chemistry-climate model EMAC. The formation processes of ice crystals considered are ice nucleation in the cirrus regime (NCIR), ice nucleation in the mixed-

phase regime (NMIX), secondary ice production (represented via the Hallet-Mossop process, SECP), convective detrainment (DETR), and instantaneous freezing of supercooled ~~cloud droplets in liquid-origin cirrus clouds~~, water cloud droplets (FREE).  
530 The loss processes of ice crystals are melting (MELT), self-collection, ~~aggregation~~ (SELF), aggregation (AGGR), and accretion ~~. Sedimentation was considered to be a source or sink according to its sign~~ (ACCR).

~~We found that orography, dust and anthropogenic particle availability, and land-ocean differences determine much of the spatial variability in the tendency fields. We defined the hierarchy of~~ also evaluated the model in-cloud ICNC with satellite ICNC retrievals by the DARDAR-Nice data set. The comparison showed that EMAC reproduces the main features of the global  
535 ICNC distribution and the zonal ICNC profile, although there are differences in terms of absolute values. Like other models, EMAC overestimates ICNC in the cirrus regime in the extratropics, perhaps because of the instantaneous freezing process; on the other hand, ICNC is underestimated in the mixed-phase regime. One possible reason could be the low freezing threshold assumed for convective detrainment.

We analysed the global distributions and means of all microphysical tendencies, in particular defining a hierarchy of ice  
540 crystal sources and sinks ~~of ice crystals at the global scale~~. We found that, on average, the hierarchy of the IC sources is FREE > ~~SEDI~~ > DETR > NCIR > NMIX > SECP, while the hierarchy of the IC sinks is AGGR > ~~SEDI~~ > ACCR > SELF > MELT. The fact that freezing is the largest source of ICs, followed by detrainment, is in agreement with the results of Muench and Lohmann (2020), although they parameterized freezing differently, taking into account its dependence on updraft velocity. Wernli et al. (2016) and Krämer et al. (2016) also found a predominance of liquid-origin cirrus over in-situ cirrus. We  
545 therefore reiterate that more efforts should be devoted to improve liquid-origin cirrus clouds (Muench and Lohmann, 2020). In the case of the CLOUD submodel, for example, FREE consists in a direct conversion of cloud droplets into ICs while it should not depend only on CDNC (Kärcher and Seifert, 2016), so it is likely that FREE is overestimated in CLOUD. A better FREE parameterization should reduce the overestimation of ICNC with respect to observations, as indicated by our test simulation NOfree. The distributions of the tendencies are left-skewed. We found that the distribution of MELT is close to a bell-shaped  
550 distribution and the ones of SELF, AGGR, and ACCR are trimodal.

~~Regionally, the relative importance of the microphysical processes can be different. For example, convective detrainment is more important than sedimentation over the Sahara and Amazon (regions at low latitudes), while~~ Numerical tendencies can have a non-negligible contribution to ICNC (Table 2 and Figure 3). The largest numerical tendency is negative and imposes an upper threshold of ICNC ( $10^7 \text{ m}^{-3}$ ). Our test simulation NOicncmax proved the strong effect of such numerical tendency  
555 in reducing ICNC. Working to reduce numerical tendencies is important because they could obscure the ice microphysical parameterization results. Such improvements would require using observations to infer active ice microphysical processes from, for example, crystal size distributions and the surrounding thermodynamic conditions and ensuring that the same processes are triggered in the model.

~~Regionally, the relative importance of the microphysical sources can vary, while the sinks appear similar. For example, heterogeneous nucleation in the mixed-phase regime is slightly more important than NCIR over the Sahara, and Europe because of the role of mineral dust as INP. ICNCs peak at lower altitudes over the oceans and mid-latitude regions than over the tropical land masses, as do their accretion and aggregation sinks and sedimentation sources.~~

The distributions of the tendencies are strongly asymmetric with most of them being close to zero and large tails (as shown by the 1st and 99th percentiles computed for sinks and sources, respectively). The asymmetry persists even when tendencies are computed in volumes of air where  $ICNC > 1 \text{ L}^{-1}$ , although the skewness is less marked in this case (not shown). abundance of INPs, while secondary ice production is more important than NMIX over the Amazon. Over the oceans, tendencies are similar even in different hemispheres, subject to different aerosol conditions.

Additionally, we found that the application of different parameterizations for ice nucleation changed the ice nucleation tendencies but affected only slightly the hierarchy of the IC sources propagated only weakly to the other source and sink tendencies. Our sensitivity test suggests that the tendency hierarchy could change using different parameterizations for other microphysical processes but also another model setup. The large variation in ICNC output from these nucleation parameterizations highlights the ice nucleation parameterizations corroborates the importance of including the competition for water vapor between INPs and pre-existing ice crystals (Bacer et al., 2018).

We also computed the tendencies in a future climate (using the RCP6.0 scenario). Our results showed shows an upward shift of the freezing level and the associated microphysical processes to higher altitudes, consistent with a reduced lapse rate that is expected to and deepened troposphere that accompany surface temperature warming. The tendencies increase in the cirrus regime (NCIR and DETR especially Detrainment increases at the highest levels in the tropics, as overshooting convection may occur more often or extend deeper, in agreement with a decrease in the mean upper-level divergence, while it decreases around the freezing level, where we found a decrease in mean cloud fraction across latitudinal bands. Ice nucleation decreases in the upper troposphere) where their radiative effect is largest; however, they are found to undergo an overall reduction at the global scale, due to weaker vertical updrafts. Finally, we found an increase in upper-level ICNC in the FUT simulation causing an increase of the longwave radiative heating, which stabilizes the atmosphere. Globally, mean ICNC decreased by almost 30% in the warming scenario.

Knowing the relative importance of the microphysical process rates is of fundamental importance to assign priority to the development of microphysics parameterizations. Model improvements could benefit from the development of techniques that infer active ice microphysical processes from in-situ and remote sensing observations. Numerical tendencies can play a non-negligible role, and effort should be spent on minimizing the contribution of these. Moreover, the quantification of tendencies is essential to compare model output and observations which have different temporal resolutions.

In future studies of about the relative importance of the cold cloud microphysical processes, it would be useful to perform a similar analyses-analysis for the mass tendencies, i.e. the rates of cloud ice mixing ratios. Moreover, the transport tendencies could be included. The transport and sedimentation tendencies could also be included to close the ICNC budget. Finally, since cloud lifetime can be short, of the order of hours, it would be interesting to perform ensemble runs in order to test the sensitivity of the results to different output frequencies and also to various model resolutions.

*Data availability.* The simulation data used in this study are available upon request.



595 *Author contributions.* SB performed the model simulations with AP. SB analysed the data together with SS, OS, and AP. SB prepared the manuscript together with SS and SO. All the authors provided assistance in finalizing the analysis and the manuscript.

*Competing interests.* The authors declare that they have no conflict of interest.

*Acknowledgements.* ~~We~~ The authors would like to thank the reviewers for their comments, which helped to improve the analysis in this study. Also, the authors would like to thank ~~Sergey Gromov~~ Steffen Münch from the ETH Zürich, Sergey Gromov and Klaus Klingmüller from the Max Planck Institute for Chemistry ~~for the discussion on the model results~~ (MPIC), and Mattia Righi from the Deutsches Zentrum für Luft- und Raumfahrt (DLR) for the useful discussions. SS was funded by the DFG project TropiC in collaboration with NSF PIRE project 1743753. HT acknowledges funding from the Carl-Zeiss foundation. We acknowledge the usage of the Max Planck Computing and Data Facility (MPCDF) for the simulations performed in this work.

600



## References

- 605 Bacer, S., Sullivan, S. C., Karydis, V. A., Barahona, D., Krämer, M., Nenes, A., Tost, H., Tsimpidi, A. P., Lelieveld, J., and Pozzer, A.: Implementation of a comprehensive ice crystal formation parameterization for cirrus and mixed-phase clouds in the EMAC model (based on MESSy 2.53), *Geoscientific Model Development*, 11, 4021–4041, <https://doi.org/10.5194/gmd-11-4021-2018>, <https://www.geosci-model-dev.net/11/4021/2018/>, 2018.
- Barahona, D. and Nenes, A.: Parameterization of cirrus cloud formation in large-scale models: Homogeneous nucleation, *Journal of Geophysical Research: Atmospheres*, 113, n/a–n/a, <https://doi.org/10.1029/2007JD009355>, d11211, 2008.
- 610 Barahona, D. and Nenes, A.: Parameterizing the competition between homogeneous and heterogeneous freezing in ice cloud formation - polydisperse ice nuclei, *Atmospheric Chemistry and Physics*, 9, 5933–5948, <https://doi.org/10.5194/acp-9-5933-2009>, <https://www.atmos-chem-phys.net/9/5933/2009/>, 2009.
- Barahona, D., Molod, A., Bacmeister, J., Nenes, A., Gettelman, A., Morrison, H., Phillips, V., and Eichmann, A.: Development of two-moment cloud microphysics for liquid and ice within the NASA Goddard Earth Observing System Model (GEOS-5), *Geoscientific Model Development*, 7, 1733–1766, <https://doi.org/10.5194/gmd-7-1733-2014>, <https://www.geosci-model-dev.net/7/1733/2014/>, 2014.
- 615 Bony, S., Stevens, B., Coppin, D., Becker, T., Reed, K. A., Voigt, A., and Medeiros, B.: Thermodynamic control of anvil cloud amount, *Proceedings of the National Academy of Sciences*, 113, 8927–8932, <https://doi.org/10.1073/pnas.1601472113>, <https://www.pnas.org/content/113/32/8927>, 2016.
- 620 Brinkop, S. and Roeckner, E.: Sensitivity of a general circulation model to parameterizations of cloud–turbulence interactions in the atmospheric boundary layer, *Tellus A*, 47, 197–220, <https://doi.org/10.1034/j.1600-0870.1995.t01-1-00004.x>, 1995.
- Cantrell, W. and Heymsfield, A.: Production of Ice in Tropospheric Clouds: A Review, *Bulletin of the American Meteorological Society*, 86, 795–807, <https://doi.org/10.1175/BAMS-86-6-795>, 2005.
- Chen, T., Rossow, W. B., and Zhang, Y.: Radiative Effects of Cloud-Type Variations, *Journal of Climate*, 13, 264–286, [https://doi.org/10.1175/1520-0442\(2000\)013<0264:REOCTV>2.0.CO;2](https://doi.org/10.1175/1520-0442(2000)013<0264:REOCTV>2.0.CO;2), 2000.
- 625 Collins, W. J., Bellouin, N., Doutriaux-Boucher, M., Gedney, N., Halloran, P., Hinton, T., Hughes, J., Jones, C. D., Joshi, M., Liddicoat, S., Martin, G., O'Connor, F., Rae, J., Senior, C., Sitch, S., Totterdell, I., Wiltshire, A., and Woodward, S.: Development and evaluation of an Earth-System model – HadGEM2, *Geosci. Model Dev.*, 4, 1051–1075, <https://doi.org/10.5194/gmd-4-1051-2011>, 2011.
- Coopman, Q., Hoose, C., and Stengel, M.: Analysis of the Thermodynamic Phase Transition of Tracked Convective Clouds Based on Geostationary Satellite Observations, *Journal of Geophysical Research: Atmospheres*, 125, e2019JD032146, <https://doi.org/10.1029/2019JD032146>, <https://agupubs.onlinelibrary.wiley.com/doi/abs/10.1029/2019JD032146>, 2020.
- 630 Del Genio, A. D., Yao, M.-S., and Jonas, J.: Will moist convection be stronger in a warmer climate?, *Geophysical Research Letters*, 34, <https://doi.org/10.1029/2007GL030525>, <https://agupubs.onlinelibrary.wiley.com/doi/abs/10.1029/2007GL030525>, 2007.
- DeMott, P. J., Prenni, A. J., Liu, X., Kreidenweis, S. M., Petters, M. D., Twohy, C. H., Richardson, M. S., Eidhammer, T., and Rogers, D. C.: Predicting global atmospheric ice nuclei distributions and their impacts on climate, *Proceedings of the National Academy of Sciences*, 107, 11 217–11 222, <https://doi.org/10.1073/pnas.0910818107>, 2010.
- 635 DeMott, P. J., Hill, T. C. J., McCluskey, C. S., Prather, K. A., Collins, D. B., Sullivan, R. C., Ruppel, M. J., Mason, R. H., Irish, V. E., Lee, T., Hwang, C. Y., Rhee, T. S., Snider, J. R., McMeeking, G. R., Dhaniyala, S., Lewis, E. R., Wentzell, J. J. B., Abbatt, J., Lee, C., Sultana, C. M., Ault, A. P., Axson, J. L., Diaz Martinez, M., Venero, I., Santos-Figueroa, G., Stokes, M. D., Deane, G. B., Mayol-Bracero, O. L., Grassian, V. H., Bertram, T. H., Bertram, A. K., Moffett, B. F., and Franc, G. D.: Sea spray aerosol as a unique source of

ice nucleating particles, *Proceedings of the National Academy of Sciences*, 113, 5797–5803, <https://doi.org/10.1073/pnas.1514034112>, <http://www.pnas.org/content/113/21/5797.abstract>, 2016.

Dietlicher, R., Neubauer, D., and Lohmann, U.: Elucidating ice formation pathways in the aerosol–climate model ECHAM6-HAM2, *Atmospheric Chemistry and Physics*, 19, 9061–9080, <https://doi.org/10.5194/acp-19-9061-2019>, <https://acp.copernicus.org/articles/19/9061/2019/>, 2019.

Dietmüller, S., Jöckel, P., Tost, H., Kunze, M., Gellhorn, C., Brinkop, S., Frömming, C., Ponater, M., Steil, B., Lauer, A., and Hendricks, J.: A new radiation infrastructure for the Modular Earth Submodel System (MESSy, based on version 2.51), *Geoscientific Model Development*, 9, 2209–2222, <https://doi.org/10.5194/gmd-9-2209-2016>, <https://www.geosci-model-dev.net/9/2209/2016/>, 2016.

Field, P. R., Lawson, R. P., Brown, P. R. A., Lloyd, G., Westbrook, C., Moisseev, D., Miltenberger, A., Nenes, A., Blyth, A., Choulaton, T., Connolly, P., Buehl, J., Crosier, J., Cui, Z., Dearden, C., DeMott, P., Flossmann, A., Heymsfield, A., Huang, Y., Kalesse, H., Kanji, Z. A., Korolev, A., Kirchgaessner, A., Lasher-Trapp, S., Leisner, T., McFarquhar, G., Phillips, V., Stith, J., and Sullivan, S.: Secondary Ice Production: Current State of the Science and Recommendations for the Future, *Meteorological Monographs*, 58, 7.1–7.20, <https://doi.org/10.1175/AMSMONOGRAPHIS-D-16-0014.1>, 2017.

Fujino, J., Nair, R., Kainuma, M., Masui, T., and Matsuoka, Y.: Multi-gas Mitigation Analysis on Stabilization Scenarios Using Aim Global Model, *The Energy Journal*, 3, 343–354, 2006.

Gasparini, B. and Lohmann, U.: Why cirrus cloud seeding cannot substantially cool the planet, *Journal of Geophysical Research: Atmospheres*, 121, 4877–4893, <https://doi.org/10.1002/2015JD024666>, 2016.

Gottelman, A., Morrison, H., Terai, C. R., and Wood, R.: Microphysical process rates and global aerosol–cloud interactions, *Atmospheric Chemistry and Physics*, 13, 9855–9867, <https://doi.org/10.5194/acp-13-9855-2013>, <https://www.atmos-chem-phys.net/13/9855/2013/>, 2013.

Gryspeerd, E., Sourdeval, O., Quaas, J., Delanoë, J., Krämer, M., and Kühne, P.: Ice crystal number concentration estimates from lidar–radar satellite remote sensing – Part 2: Controls on the ice crystal number concentration, *Atmospheric Chemistry and Physics*, 18, 14 351–14 370, <https://doi.org/10.5194/acp-18-14351-2018>, <https://www.atmos-chem-phys.net/18/14351/2018/>, 2018.

Guo, H., Liu, Y., Daum, P. H., Senum, G. I., and Tao, W.-K.: Characteristics of vertical velocity in marine stratocumulus: comparison of large eddy simulations with observations, *Environmental Research Letters*, 3, 1–8, <https://doi.org/10.1088/1748-9326/3/4/045020>, 2008.

Hallett, J. and Mossop, S. C.: Production of secondary ice particles during the riming process, *Nature*, 249, 26–28, <https://doi.org/10.1038/249026a0>, 1974.

Heymsfield, A. J., Krämer, M., Luebke, A., Brown, P., Cziczo, D. J., Franklin, C., Lawson, P., Lohmann, U., McFarquhar, G., Ulanowski, Z., and Van Tricht, K.: Cirrus Clouds, *Meteorological Monographs*, 58, 2.1–2.26, <https://doi.org/10.1175/AMSMONOGRAPHIS-D-16-0010.1>, 2017.

Hong, Y., Liu, G., and Li, J.-L. F.: Assessing the Radiative Effects of Global Ice Clouds Based on CloudSat and CALIPSO Measurements, *Journal of Climate*, 29, 7651–7674, <https://doi.org/10.1175/JCLI-D-15-0799.1>, 2016.

Hoose, C., Kristjánsson, J. E., and Burrows, S. M.: How important is biological ice nucleation in clouds on a global scale?, *Environmental Research Letters*, 5, 024 009, <http://stacks.iop.org/1748-9326/5/i=2/a=024009>, 2010.

IPCC: Climate Change 2013: The Physical Science Basis, Cambridge University Press, 1535 pp., 2013.

Jensen, E. J., Diskin, G., Lawson, R. P., Lance, S., Bui, T. P., Hlavka, D., McGill, M., Pfister, L., Toon, O. B., and Gao, R.: Ice nucleation and dehydration in the Tropical Tropopause Layer, *Proceedings of the National Academy of Sciences*, 110, 2041–2046, <https://doi.org/10.1073/pnas.1217104110>, <http://www.pnas.org/content/110/6/2041>, 2013.

Jöckel, P., Kerkweg, A., Pozzer, A., Sander, R., Tost, H., Riede, H., Baumgaertner, A., Gromov, S., and Kern, B.: Development cycle 2 of the Modular Earth Submodel System (MESSy2), *Geoscientific Model Development*, 3, 717–752, <https://doi.org/10.5194/gmd-3-717-2010>, <https://www.geosci-model-dev.net/3/717/2010/>, 2010.

Jöckel, P., Tost, H., Pozzer, A., Kunze, M., Kirner, O., Brenninkmeijer, C. A. M., Brinkop, S., Cai, D. S., Dyroff, C., Eckstein, J., Frank, F., Garny, H., Gottschaldt, K.-D., Graf, P., Grewe, V., Kerkweg, A., Kern, B., Matthes, S., Mertens, M., Meul, S., Neumaier, M., Nützel, M., Oberländer-Hayn, S., Ruhnke, R., Runde, T., Sander, R., Scharffe, D., and Zahn, A.: Earth System Chemistry integrated Modelling (ESCiMo) with the Modular Earth Submodel System (MESSy) version 2.51, *Geoscientific Model Development*, 9, 1153–1200, <https://doi.org/10.5194/gmd-9-1153-2016>, <https://www.geosci-model-dev.net/9/1153/2016/>, 2016.

Kanji, Z. A., Ladino, L. A., Wex, H., Boose, Y., Burkert-Kohn, M., Cziczo, D. J., and Krämer, M.: Overview of Ice Nucleating Particles, *Meteorological Monographs*, 58, 1.1–1.33, <https://doi.org/10.1175/AMSMONOGRAPHIS-D-16-0006.1>, 2017.

Kärcher, B. and Lohmann, U.: A parameterization of cirrus cloud formation: Homogeneous freezing of supercooled aerosols, *Journal of Geophysical Research: Atmospheres*, 107, AAC 4–1–AAC 4–10, <https://doi.org/10.1029/2001JD000470>, 2002a.

Kärcher, B. and Lohmann, U.: A Parameterization of cirrus cloud formation: Homogeneous freezing including effects of aerosol size, *Journal of Geophysical Research: Atmospheres*, 107, AAC 9–1–AAC 9–10, <https://doi.org/10.1029/2001JD001429>, 2002b.

Kärcher, B. and Seifert, A.: On homogeneous ice formation in liquid clouds, *Quarterly Journal of the Royal Meteorological Society*, 142, 1320–1334, <https://doi.org/https://doi.org/10.1002/qj.2735>, <https://rmets.onlinelibrary.wiley.com/doi/abs/10.1002/qj.2735>, 2016.

Karydis, V. A., Kumar, P., Barahona, D., Sokolik, I. N., and Nenes, A.: On the effect of dust particles on global cloud condensation nuclei and cloud droplet number, *Journal of Geophysical Research: Atmospheres*, 116, <https://doi.org/10.1029/2011JD016283>, d23204, 2011.

Karydis, V. A., Tsimpidi, A. P., Pozzer, A., Astitha, M., and Lelieveld, J.: Effects of mineral dust on global atmospheric nitrate concentrations, *Atmospheric Chemistry and Physics*, 16, 1491–1509, <https://doi.org/10.5194/acp-16-1491-2016>, <https://www.atmos-chem-phys.net/16/1491/2016/>, 2016.

Karydis, V. A., Tsimpidi, A. P., Bacer, S., Pozzer, A., Nenes, A., and Lelieveld, J.: Global impact of mineral dust on cloud droplet number concentration, *Atmospheric Chemistry and Physics*, 17, 5601–5621, <https://doi.org/10.5194/acp-17-5601-2017>, <https://www.atmos-chem-phys.net/17/5601/2017/>, 2017.

Kerkweg, A., Buchholz, J., Ganzeveld, L., Pozzer, A., Tost, H., and Jöckel, P.: Technical Note: An implementation of the dry removal processes DRY DEPosition and SEDimentation in the Modular Earth Submodel System (MESSy), *Atmospheric Chemistry and Physics*, 6, 4617–4632, <https://doi.org/10.5194/acp-6-4617-2006>, <https://www.atmos-chem-phys.net/6/4617/2006/>, 2006a.

Kerkweg, A., Sander, R., Tost, H., and Jöckel, P.: Technical note: Implementation of prescribed (OFFLEM), calculated (ONLEM), and pseudo-emissions (TNUDGE) of chemical species in the Modular Earth Submodel System (MESSy), *Atmospheric Chemistry and Physics*, 6, 3603–3609, <https://doi.org/10.5194/acp-6-3603-2006>, <https://www.atmos-chem-phys.net/6/3603/2006/>, 2006b.

Khain, A. P. and Pinsky, M.: *Physical processes in clouds and in cloud modeling*, Cambridge University Press, 2018.

Klingmüller, K., Metzger, S., Abdelkader, M., Karydis, V. A., Stenchikov, G. L., Pozzer, A., and Lelieveld, J.: Revised mineral dust emissions in the atmospheric chemistry-climate model EMAC (MESSy 2.52 DU\_Astitha1KKDU2017 patch), *Geoscientific Model Development Discussions*, 11, 989–1008, <https://doi.org/10.5194/gmd-11-989-2018>, 2018.

Korolev, A., McFarquhar, G., Field, P. R., Franklin, C., Lawson, P., Wang, Z., Williams, E., Abel, S. J., Axisa, D., Borrmann, S., Crosier, J., Fugal, J., Krämer, M., Lohmann, U., Schlenczek, O., Schnaiter, M., and Wendisch, M.: Mixed-Phase Clouds: Progress and Challenges, *Meteorological Monographs*, 58, 5.1–5.50, <https://doi.org/10.1175/AMSMONOGRAPHIS-D-17-0001.1>, 2017.

- Krämer, M., Rolf, C., Luebke, A., Afchine, A., Spelten, N., Costa, A., Meyer, J., Zöger, M., Smith, J., Herman, R. L., Buchholz, B., Ebert, V., Baumgardner, D., Borrmann, S., Klingebiel, M., and Avallone, L.: A microphysics guide to cirrus clouds – Part 1: Cirrus types, *Atmospheric Chemistry and Physics*, 16, 3463–3483, <https://doi.org/10.5194/acp-16-3463-2016>, <https://www.atmos-chem-phys.net/16/3463/2016/>, 2016.
- 720 Krämer, M., Rolf, C., Spelten, N., Afchine, A., Fahey, D., Jensen, E., Khaykin, S., Kuhn, T., Lawson, P., Lykov, A., Pan, L. L., Riese, M., Rollins, A., Stroh, F., Thornberry, T., Wolf, V., Woods, S., Spichtinger, P., Quaas, J., and Sourdeval, O.: A microphysics guide to cirrus – Part 2: Climatologies of clouds and humidity from observations, *Atmospheric Chemistry and Physics*, 20, 12 569–12 608, <https://doi.org/10.5194/acp-20-12569-2020>, <https://acp.copernicus.org/articles/20/12569/2020/>, 2020.
- Kuebbeler, M., Lohmann, U., Hendricks, J., and Kärcher, B.: Dust ice nuclei effects on cirrus clouds, *Atmospheric Chemistry and Physics*, 725 14, 3027–3046, <https://doi.org/10.5194/acp-14-3027-2014>, <https://www.atmos-chem-phys.net/14/3027/2014/>, 2014.
- Kumar, P., Sokolik, I. N., and Nenes, A.: Parameterization of cloud droplet formation for global and regional models: including adsorption activation from insoluble CCN, *Atmospheric Chemistry and Physics*, 9, 2517–2532, <https://doi.org/10.5194/acp-9-2517-2009>, <https://www.atmos-chem-phys.net/9/2517/2009/>, 2009.
- Kumar, P., Sokolik, I. N., and Nenes, A.: Cloud condensation nuclei activity and droplet activation kinetics of wet processed regional 730 dust samples and minerals, *Atmospheric Chemistry and Physics*, 11, 8661–8676, <https://doi.org/10.5194/acp-11-8661-2011>, <https://www.atmos-chem-phys.net/11/8661/2011/>, 2011.
- Lamarque, J.-F., Bond, T. C., Eyring, V., Granier, C., Heil, A., Klimont, Z., Lee, D., Lioussé, C., Mieville, A., Owen, B., Schultz, M. G., Shindell, D., Smith, S. J., Stehfest, E., Van Aardenne, J., Cooper, O. R., Kainuma, M., Mahowald, N., McConnell, J. R., Naik, V., Riahi, K., and van Vuuren, D. P.: Historical (1850–2000) gridded anthropogenic and biomass burning emissions of reactive gases and 735 aerosols: methodology and application, *Atmospheric Chemistry and Physics*, 10, 7017–7039, <https://doi.org/10.5194/acp-10-7017-2010>, <https://www.atmos-chem-phys.net/10/7017/2010/>, 2010.
- Lawson, R. P., Woods, S., Jensen, E., Erfani, E., Gurganus, C., Gallagher, M., Connolly, P., Whiteway, J., Baran, A. J., May, P., Heymsfield, A., Schmitt, C. G., McFarquhar, G., Um, J., Protat, A., Bailey, M., Lance, S., Muehlbauer, A., Stith, J., Korolev, A., Toon, O. B., and Krämer, M.: A Review of Ice Particle Shapes in Cirrus formed In Situ and in Anvils, *Journal of Geophysical Research: Atmospheres*, 124, 740 10 049–10 090, <https://doi.org/10.1029/2018JD030122>, <https://agupubs.onlinelibrary.wiley.com/doi/abs/10.1029/2018JD030122>, 2019.
- Levkov, L., Rockel, B., Kapitza, H., and E., R.: 3D mesoscale numerical studies of cirrus and stratus clouds by their time and space evolution, *Beitr. Phys. Atmos*, 65, 35–58, 1992.
- Lin, Y.-L., Farley, R. D., and Orville, H. D.: Bulk Parameterization of the Snow Field in a Cloud Model, *Journal of Climate and Applied Meteorology*, 22, 1065–1092, [https://doi.org/10.1175/1520-0450\(1983\)022<1065:BPOTSF>2.0.CO;2](https://doi.org/10.1175/1520-0450(1983)022<1065:BPOTSF>2.0.CO;2), 1983.
- 745 Liu, X., Shi, X., Zhang, K., Jensen, E. J., Gettelman, A., Barahona, D., Nenes, A., and Lawson, P.: Sensitivity studies of dust ice nuclei effect on cirrus clouds with the Community Atmosphere Model CAM5, *Atmospheric Chemistry and Physics*, 12, 12 061–12 079, <https://doi.org/10.5194/acp-12-12061-2012>, <https://www.atmos-chem-phys.net/12/12061/2012/>, 2012.
- Lohmann, U.: Possible Aerosol Effects on Ice Clouds via Contact Nucleation, *Journal of the Atmospheric Sciences*, 59, 647–656, [https://doi.org/10.1175/1520-0469\(2001\)059<0647:PAEOIC>2.0.CO;2](https://doi.org/10.1175/1520-0469(2001)059<0647:PAEOIC>2.0.CO;2), 2002.
- 750 Lohmann, U.: Can Anthropogenic Aerosols Decrease the Snowfall Rate?, *Journal of the Atmospheric Sciences*, 61, 2457–2468, [https://doi.org/10.1175/1520-0469\(2004\)061<2457:CAADTS>2.0.CO;2](https://doi.org/10.1175/1520-0469(2004)061<2457:CAADTS>2.0.CO;2), [https://doi.org/10.1175/1520-0469\(2004\)061<2457:CAADTS>2.0.CO;2](https://doi.org/10.1175/1520-0469(2004)061<2457:CAADTS>2.0.CO;2), 2004.

- Lohmann, U. and Diehl, K.: Sensitivity Studies of the Importance of Dust Ice Nuclei for the Indirect Aerosol Effect on Stratiform Mixed-Phase Clouds, *Journal of the Atmospheric Sciences*, 63, 968–982, <https://doi.org/10.1175/JAS3662.1>, 2006.
- 755 Lohmann, U. and Gasparini, B.: A cirrus cloud climate dial?, *Science*, 357, 248–249, <https://doi.org/10.1126/science.aan3325>, <https://science.sciencemag.org/content/357/6348/248>, 2017.
- Lohmann, U. and Kärcher, B.: First interactive simulations of cirrus clouds formed by homogeneous freezing in the ECHAM general circulation model, *Journal of Geophysical Research: Atmospheres*, 107, AAC 8–1–AAC 8–13, <https://doi.org/10.1029/2001JD000767>, 2002.
- Lohmann, U., Feichter, J., Chuang, C. C., and Penner, J. E.: Prediction of the number of cloud droplets in the ECHAM GCM, *Journal of*  
760 *Geophysical Research: Atmospheres*, 104, 9169–9198, <https://doi.org/10.1029/1999JD900046>, 1999.
- Lohmann, U., Stier, P., Hoose, C., Ferrachat, S., Kloster, S., Roeckner, E., and Zhang, J.: Cloud microphysics and aerosol indirect effects in the global climate model ECHAM5-HAM, *Atmospheric Chemistry and Physics*, 7, 3425–3446, <https://doi.org/10.5194/acp-7-3425-2007>, <https://www.atmos-chem-phys.net/7/3425/2007/>, 2007.
- Matus, A. V. and L'Ecuyer, T. S.: The role of cloud phase in Earth's radiation budget, *Journal of Geophysical Research: Atmospheres*, 122,  
765 2559–2578, <https://doi.org/10.1002/2016JD025951>, 2017.
- Muench, S. and Lohmann, U.: Developing a Cloud Scheme With Prognostic Cloud Fraction and Two Moment Microphysics for ECHAM-HAM, *Journal of Advances in Modeling Earth Systems*, 12, e2019MS001 824, <https://doi.org/10.1029/2019MS001824>, <https://agupubs.onlinelibrary.wiley.com/doi/abs/10.1029/2019MS001824>, 2020.
- Nordeng, T. E.: Extended versions of the convection parametrization scheme at ECMWF and their impact upon the mean climate and transient  
770 activity of the model in the tropics, ECMWF Tech. Memo. No. 206, 1994.
- Petters, M. D. and Kreidenweis, S. M.: A single parameter representation of hygroscopic growth and cloud condensation nucleus activity, *Atmospheric Chemistry and Physics*, 7, 1961–1971, <https://doi.org/10.5194/acp-7-1961-2007>, <https://www.atmos-chem-phys.net/7/1961/2007/>, 2007.
- Phillips, V. T. J., Donner, L. J., and Garner, S. T.: Nucleation Processes in Deep Convection Simulated by a Cloud-System-Resolving Model  
775 with Double-Moment Bulk Microphysics, *Journal of the Atmospheric Sciences*, 64, 738–761, <https://doi.org/10.1175/JAS3869.1>, 2007.
- Phillips, V. T. J., Demott, P. J., Andronache, C., Pratt, K. A., Prather, K. A., Subramanian, R., and Twohy, C.: Improvements to an Empirical Parameterization of Heterogeneous Ice Nucleation and Its Comparison with Observations, *Journal of the Atmospheric Sciences*, 70, 378–409, <https://doi.org/10.1175/JAS-D-12-080.1>, 2013.
- Pozzer, A., de Meij, A., Pringle, K. J., Tost, H., Doering, U. M., van Aardenne, J., and Lelieveld, J.: Distributions and regional budgets  
780 of aerosols and their precursors simulated with the EMAC chemistry-climate model, *Atmospheric Chemistry and Physics*, 12, 961–987, <https://doi.org/10.5194/acp-12-961-2012>, <https://www.atmos-chem-phys.net/12/961/2012/>, 2012.
- Pozzer, A., de Meij, A., Yoon, J., Tost, H., Georgoulias, A. K., and Astitha, M.: AOD trends during 2001–2010 from observations and model simulations, *Atmospheric Chemistry and Physics*, 15, 5521–5535, <https://doi.org/10.5194/acp-15-5521-2015>, <https://www.atmos-chem-phys.net/15/5521/2015/>, 2015.
- 785 Pringle, K. J., Tost, H., Message, S., Steil, B., Giannadaki, D., Nenes, A., Fountoukis, C., Stier, P., Vignati, E., and Lelieveld, J.: Description and evaluation of GMX<sub>e</sub>: a new aerosol submodel for global simulations (v1), *Geoscientific Model Development*, 3, 391–412, <https://doi.org/10.5194/gmd-3-391-2010>, <https://www.geosci-model-dev.net/3/391/2010/>, 2010.
- Pruppacher, H. R. and Klett, J. D.: *Microphysics of Clouds and Precipitation*, Springer, New York, 954 pp, 1997.
- Roeckner, E., Brokopf, R., Esch, M., Giorgetta, M., Hagemann, S., Kornblueh, L., Schlese, U., Schulzweida, U., and Manzini, E.: The  
790 *Atmospheric General Circulation Model ECHAM5, Part II*, Max-Planck-Institut für Meteorologie, p. 25, 2004.

- Roeckner, E., Brokopf, R., Esch, M., Giorgetta, M., Hagemann, S., Kornblüeh, L., Manzini, E., Schlese, U., and Schulzweida, U.: Sensitivity of Simulated Climate to Horizontal and Vertical Resolution in the ECHAM5 Atmosphere Model, *Journal of Climate*, 19, 3771–3791, <https://doi.org/10.1175/JCLI3824.1>, 2006.
- Rogers, R. R. and Yau, M. K.: *A short course in cloud physics*, Butterworth-Heinemann, 3rd edn., 1989.
- 795 Sander, R., Baumgaertner, A., Gromov, S., Harder, H., Jöckel, P., Kerkweg, A., Kubistin, D., Regelin, E., Riede, H., Sandu, A., Taraborrelli, D., Tost, H., and Xie, Z.-Q.: The atmospheric chemistry box model CAABA/MECCA-3.0, *Geoscientific Model Development*, 4, 373–380, <https://doi.org/10.5194/gmd-4-373-2011>, <https://www.geosci-model-dev.net/4/373/2011/>, 2011.
- Sanderson, B. M., Piani, C., Ingram, W. J., A., S. D., and R., A. M.: Towards constraining climate sensitivity by linear analysis of feedback patterns in thousands of perturbed-physics GCM simulations, *Climate Dynamics*, 30, 175–190, [https://doi.org/10.1007/s00382-007-0280-](https://doi.org/10.1007/s00382-007-0280-7)  
800 7, 2008.
- Seinfeld, J. H., Bretherton, C., Carslaw, K. S., Coe, H., DeMott, P. J., Dunlea, E. J., Feingold, G., Ghan, S., Guenther, A. B., Kahn, R., Kraucunas, I., Kreidenweis, S. M., Molina, M. J., Nenes, A., Penner, J. E., Prather, K. A., Ramanathan, V., Ramaswamy, V., Rasch, P. J., Ravishankara, A. R., Rosenfeld, D., Stephens, G., and Wood, R.: Improving our fundamental understanding of the role of aerosol-cloud interactions in the climate system, *Proceedings of the National Academy of Sciences*, 113, 5781–5790, <https://doi.org/10.1073/pnas.1514043113>,  
805 <http://www.pnas.org/content/113/21/5781>, 2016.
- Sourdeval, O., Gryspeerdt, E., Krämer, M., Goren, T., Delanoë, J., Afchine, A., Hemmer, F., and Quaas, J.: Ice crystal number concentration estimates from lidar–radar satellite remote sensing – Part 1: Method and evaluation, *Atmospheric Chemistry and Physics*, 18, 14 327–14 350, <https://doi.org/10.5194/acp-18-14327-2018>, <https://www.atmos-chem-phys.net/18/14327/2018/>, 2018.
- Sullivan, S. C., Morales Betancourt, R., Barahona, D., and Nenes, A.: Understanding cirrus ice crystal number variability for different  
810 heterogeneous ice nucleation spectra, *Atmospheric Chemistry and Physics*, 16, 2611–2629, <https://doi.org/10.5194/acp-16-2611-2016>, <https://www.atmos-chem-phys.net/16/2611/2016/>, 2016.
- Sullivan, S. C., Barthlott, C., Crosier, J., Zhukov, I., Nenes, A., and Hoose, C.: The effect of secondary ice production parameterization on the simulation of a cold frontal rainband, *Atmospheric Chemistry and Physics*, 18, 16 461–16 480, [https://doi.org/10.5194/acp-18-16461-](https://doi.org/10.5194/acp-18-16461-2018)  
2018, <https://www.atmos-chem-phys.net/18/16461/2018/>, 2018a.
- 815 Sullivan, S. C., Hoose, C., Kiselev, A., Leisner, T., and Nenes, A.: Initiation of secondary ice production in clouds, *Atmospheric Chemistry and Physics*, 18, 1593–1610, <https://doi.org/10.5194/acp-18-1593-2018>, <https://www.atmos-chem-phys.net/18/1593/2018/>, 2018b.
- Sundqvist, H., Berge, E., and Kristjansson, J. E.: *Condensation and Cloud Parameterization Studies with a Mesoscale Numerical Weather Prediction Model*, *Monthly Weather Review*, 117, 1641–1657, 1989.
- Tiedtke, M.: A Comprehensive Mass Flux Scheme for Cumulus Parameterization in Large-Scale Models, *Monthly Weather Review*, 117,  
820 1779–1800, [https://doi.org/10.1175/1520-0493\(1989\)117<1779:ACMFSF>2.0.CO;2](https://doi.org/10.1175/1520-0493(1989)117<1779:ACMFSF>2.0.CO;2), 1989.
- Tost, H., Jöckel, P., Kerkweg, A., Sander, R., and Lelieveld, J.: Technical note: A new comprehensive SCAVenging submodel for global atmospheric chemistry modelling, *Atmospheric Chemistry and Physics*, 6, 565–574, <https://doi.org/10.5194/acp-6-565-2006>, <https://www.atmos-chem-phys.net/6/565/2006/>, 2006a.
- Tost, H., Jöckel, P., and Lelieveld, J.: Influence of different convection parameterisations in a GCM, *Atmospheric Chemistry and Physics*, 6,  
825 5475–5493, <https://doi.org/10.5194/acp-6-5475-2006>, <https://www.atmos-chem-phys.net/6/5475/2006/>, 2006b.
- Tost, H., Lawrence, M. G., Brühl, C., Jöckel, P., Team, T. G., and Team, T. S.-O.-D.: Uncertainties in atmospheric chemistry modelling due to convection parameterisations and subsequent scavenging, *Atmospheric Chemistry and Physics*, 10, 1931–1951, <https://doi.org/10.5194/acp-10-1931-2010>, <https://www.atmos-chem-phys.net/10/1931/2010/>, 2010.

- Tsimpidi, A. P., Karydis, V. A., Pandis, S. N., and Lelieveld, J.: Global combustion sources of organic aerosols: model  
830 comparison with 84 AMS factor-analysis data sets, *Atmospheric Chemistry and Physics*, 16, 8939–8962, <https://doi.org/10.5194/acp-16-8939-2016>, <https://www.atmos-chem-phys.net/16/8939/2016/>, 2016.
- Wernli, H., Boettcher, M., Joos, H., Miltenberger, A. K., and Spichtinger, P.: A trajectory-based classification of ERA-Interim ice clouds in the region of the North Atlantic storm track, *Geophysical Research Letters*, 43, 6657–6664, <https://doi.org/10.1002/2016GL068922>, <https://agupubs.onlinelibrary.wiley.com/doi/abs/10.1002/2016GL068922>, 2016.

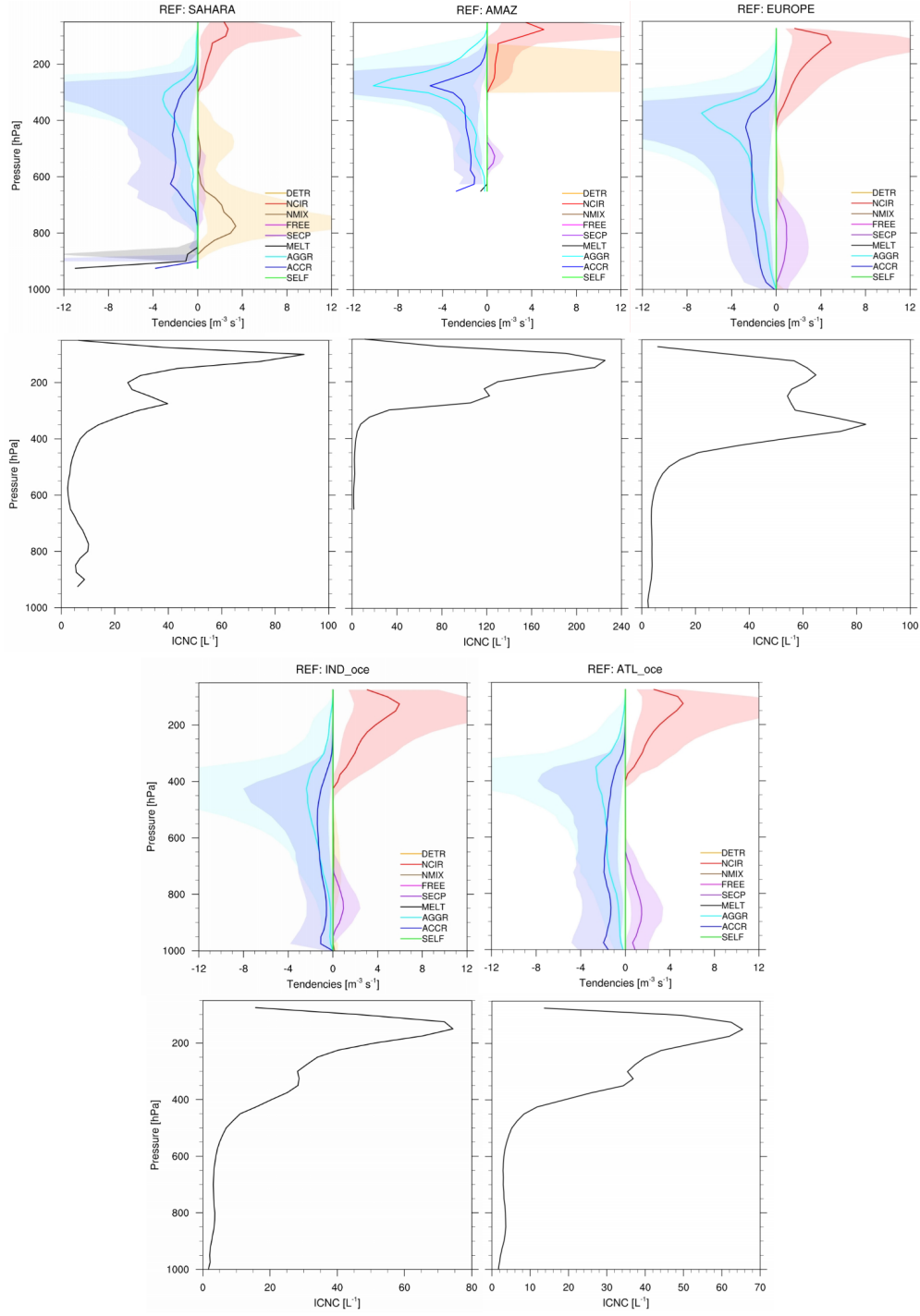


**Figure 8.** Microphysical process tendencies and ICNC as a function of pressure computed for different regions: Amazon, Sahara, Central Europe, Southern Indian Ocean, and North Atlantic Ocean. The vertical profiles are medians computed only where ICNC > 1 L<sup>-1</sup> in bins of 25 hPa. The coloured shadows mark the areas between the 25th and the 75th percentiles.



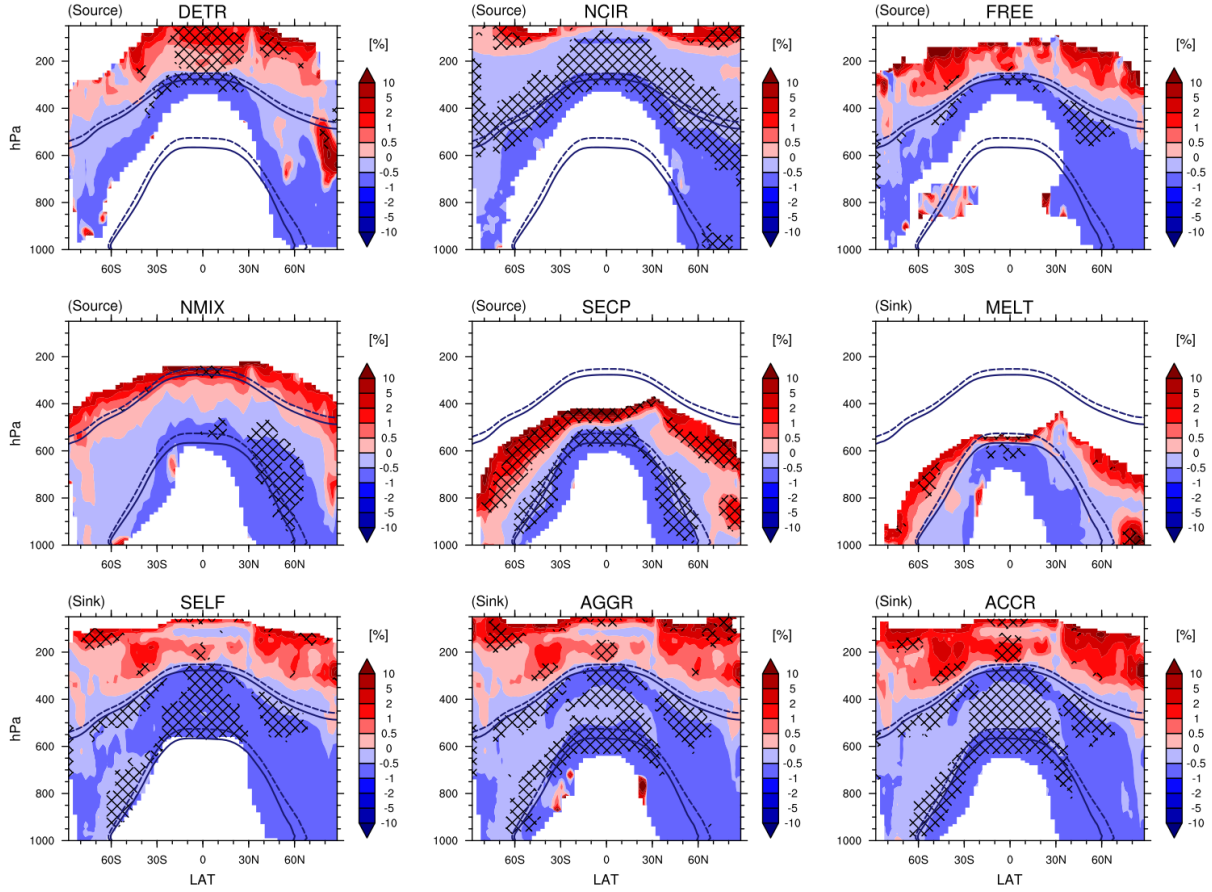


**Figure 9.** Percentage changes of the tendencies associated to ICNC microphysical processes in cold clouds in FUT with respect to REF. They are computed with daily means and are shown where REF daily means are  $> 10^{-5} \text{m}^{-3} \text{s}^{-1}$ . The hatched pattern indicates areas with a significance level of 90%. The isotherms at  $0^{\circ}\text{C}$  and  $-35^{\circ}\text{C}$  are annual means in REF (solid line) and in FUT (dashed line).

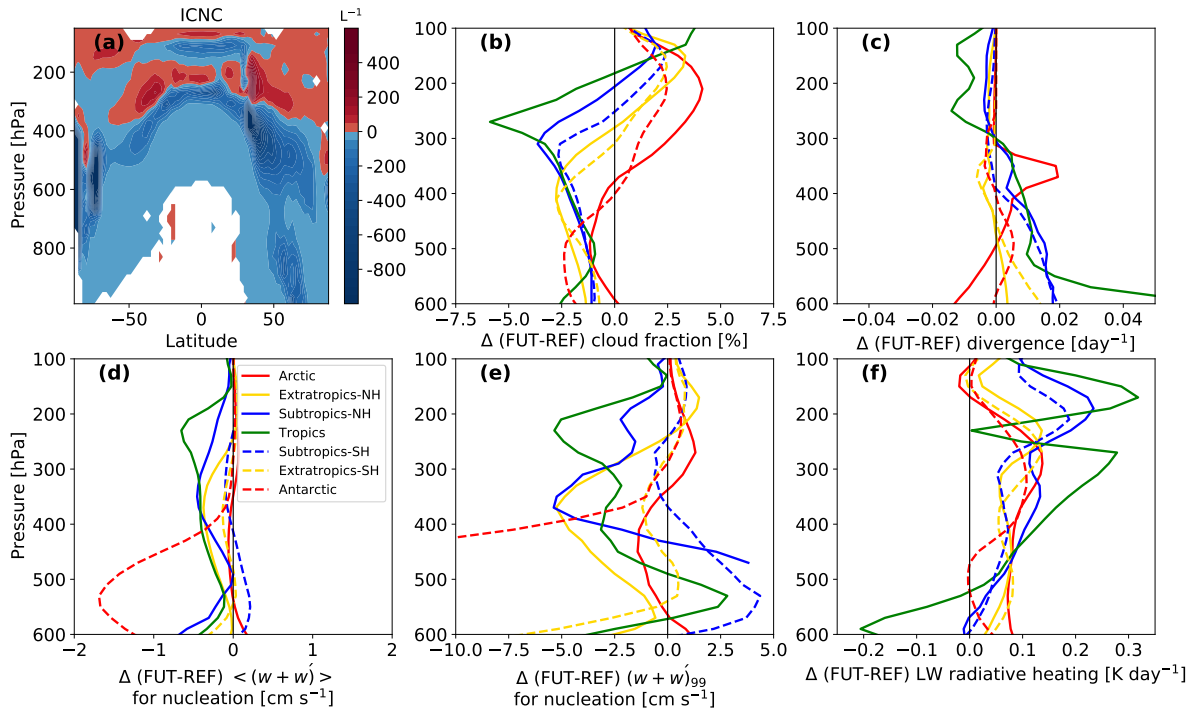


**Figure 10.** Relative percentage changes of the tendencies associated to the IC sources in cold clouds: (a) Absolute difference in ICNC between the FUT with respect to and REF simulations; (b) FUT-REF differences in the mean cloud fraction; (c) mean divergence; (d) mean input vertical velocity to the ice nucleation scheme, computed where grid-scale plus subgrid-scale variability term ( $\langle w + w' \rangle$ ); (e) extreme input vertical velocity to the ice nucleation scheme; and (f) longwave (LW) cloud radiative heating in REF and FUT simulations. The hatched pattern indicates areas with a significance level  $> 10^{-5}$ . The Arctic is defined as north of  $60^\circ$ . The isotherms at  $0^\circ\text{C}$ ,  $60^\circ\text{N}$  and  $-35^\circ\text{C}$  the Antarctic south of  $60^\circ\text{S}$ , the extratropics are annual means in REF (solid line) between  $40^\circ$  and in FUT (dashed line). (Note that SEDI here takes into account only negative values  $> 10^{-5}\text{m}^{-3}\text{s}^{-1}$  different zonal bands.)